Osteology and affinities of Dollo's goniopholidid (Mesoeucrocodylia) from the Early Cretaceous of Bernissart, Belgium

Post-print version of

Martin J. E., M. Delfino and T. Smith 2016

Osteology and affinities of Dollo's goniopholidid (Mesoeucrocodylia) from the Early Cretaceous of Bernissart, Belgium

Journal of Vertebrate Paleontology, Article: e1222534

DOI: 10.1080/02724634.2016.1222534

https://www.tandfonline.com/doi/abs/10.1080/02724634.2016.1222534?journalCode=ujvp20

Osteology and affinities of Dollo's goniopholidid (Mesoeucrocodylia) from the Early Cretaceous of Bernissart, Belgium

JEREMY E. MARTIN,[1,*] MASSIMO DELFINO,[2,3] and THIERRY SMITH[4]

[1]Univ Lyon, Ens de Lyon, Université Lyon 1, CNRS, UMR 5276 Laboratoire de Géologie de Lyon: Terre, Planète, Environnement, F-69342 Lyon, France, jeremy.martin@ens-lyon.fr

[2]Dipartimento di Scienze della Terra, Università degli Studi di Torino, via T. Valperga Caluso 35, 10125 Torino, Italy, massimo.delfino@unito.it

[3]Institut Català de Paleontologia Miquel Crusafont, Universitat Autònoma de Barcelona, Edifici Z (ICTA-ICP), Carrer de les Columnes s/n, Campus de la UAB, E-08193 Cerdanyola del Valles, Barcelona, Spain

[4]Direction opérationnelle Terre & histoire de la Vie, Institut royal des Sciences naturelles de Belgique, 29 rue Vautier, B-1000 Bruxelles, Belgium, thierry.smith@naturalsciences.be

*Corresponding author

ABSTRACT—The two specimens originally referred by Louis Dollo to *Goniopholis simus* from the Early Cretaceous of Bernissart, Belgium are described. They consist of fully articulated skeletons, one missing the skull and mandibles. Comparison of these specimens with recently revised specimens from the Wealden of England allows confirmation that the Belgian specimens are referable to the goniopholidid *Anteophthalmosuchus hooleyi*. The Belgian specimens are the most completely known representatives of this species but also of any Goniopholididae. The study of the postcranial skeletons from Bernissart reveals that the appendicular skeleton closely resembles that of derived neosuchians. The dorsal and ventral shields present a morphology directly comparable to other goniopholidids and pholidosaurids. Such observations stress on the necessity to gather an osteological database of postcranial elements to test relationships of the various neosuchian lineages. Goniopholididae were relatively diverse during the Early Cretaceous of Europe and depending on taxonomic opinion, three to five genera are recognized: *Anteophthalmosuchus*, *Goniopholis*, *Hulkepholis* and possibly *Vectisuchus* and *Nannosuchus*.

INTRODUCTION

Goniopholididae were common semi-aquatic predators in freshwater ecosystems of Laurasia during the latest Jurassic and early Cretaceous (Buffetaut, 1982). They were ecomorphologically similar to semi-aquatic eusuchians, who replaced goniopholididae only later during the Late Cretaceous (e.g. review in Martin and Delfino, 2010). Goniopholididae have been recognized in Europe, North America and Asia but are currently not recognized from southern continents (Andrade et al., 2011).

Goniopholididae have often been recovered in a derived position within Neosuchia, close to Atoposauridae or to other derived neosuchians such as

Bernissartia (Pol et al., 2009). Furthermore, *Goniopholis* spp. has sometime been used as an outgroup taxon in phylogenetic investigations of eusuchian relationships (Salisbury et al., 2006). Nevertheless, the anatomy of European goniopholidids is imperfectly known, as several features of the postcranium lack detailed descriptions. This possibly explains why no consensus has been reached over the interrelationships of Goniopholididae yet. A recent hypothesis finds Goniopholididae to cluster with Pholidosauridae (Martin and Buffetaut, 2012) inside a new taxonomic entity called Coelognathosuchia (Martin et al., 2014). More recent phylogenetic investigations of derived neosuchians recover a different topology, with Goniopholididae closer to Eusuchia than to *Isisfordia* and *Susisuchus* (Turner, 2015; Turner and Pritchard, 2015). The phylogenetic analysis presented in this paper is preliminary; this is because the unsettled interrelationships of goniopholidids within Neosuchia can only be improved when a more complete osteological framework of complete specimens representing different neosuchian lineages becomes available.

The genus *Goniopholis* Owen, 1841 is among the first Mesozoic crocodilians to have been described. Historically, species of the genus *Goniopholis* were erected from Lower Cretaceous strata (Berriasian) of England, mostly from the Purbeck Limestone Group (Owen, 1841, 1878) from relatively well-preserved cranial elements, but never from fully articulated specimens. A plethora of species have been erected on the basis of fragmentary specimens, mostly from England and the taxonomic content of this genus has been substantially diminished through time (see review in Salisbury et al., 1999). The most recent works on the taxonomy of European goniopholidids allow recognizing nine species from England, Germany, Portugal and Spain (Salisbury et al., 1999; Salisbury, 2002; Schwarz, 2002; Andrade et al., 2011; Salisbury and Naish, 2011; Buscalioni et al., 2013; Puértolas-Pascual et al., 2015;

compilation in Table 1). By the end of the XIXth century, exploitation of a coalmine at Bernissart, Belgium led to the discovery of a vertebrate assemblage containing fully articulated crocodilian skeletons including the derived neosuchian *Bernissartia fagesii* Dollo, 1883. A preliminary account of the other crocodilian material led Dollo (1883) to recognize *Goniopholis simus* by comparing it with the already known English specimen housed in NHM-UK and originally described by Owen (1878). To this date, and although Dollo (1883) had planned a full osteological study of the Bernissart *Goniopholis simus*, no detailed description has been published.

In a broad revision of *Goniopholis* (Salisbury et al., 1999), the referral of the Dollo specimens to *Goniopholis simus* has been considered invalid with Salisbury (2002) reiterating the same arguments, pointing out that differences have previously been noted by Hooley (1907) and that Dollo's specimens should be re-described and renamed. More recently, the phylogenetic analysis of Andrade et al. (2011) corroborated these claims in recovering Dollo's specimens away from *Goniopholis simus* but closely related to *Anteophthalmosuchus hooleyi* Naish and Salisbury, 2011. Salisbury and Naish (2011) noted several shared features between this new taxon and the Dollo specimens. More recently, Buscalioni et al. (2013) erected a new species, *Anteophthalmosuchus escuchae* from the early Albian of Spain. Finally, a new specimen referred to *A.* cf. *escuchae* has recently been described (Puértolas-Pascual et al., 2015).

Therefore, the purpose of this work is to provide a comprehensive osteological description of Dollo's specimens from Bernissart, Belgium, the most complete European goniopholidid; discuss their affinities with other European goniopholidids and compare cranial and postcranial features with other non-eusuchian neosuchians as a preliminary basis to discuss interrelationships of Goniopholididae.

Institutional Abbreviations—**AR**, Ariño collection, Museo Aragonés de Paleontologia, Teruel, Spain; **BMNHB**, Booth Museum of Natural History, Brighton, United Kingdom; **DORCM**, Dorset County Museum, Dorchester, United Kingdom; **IPFUB**, Institut für Paläontologie der Freien Universität, Berlin, Germany; **IRSNB**, Institut Royal des Sciences Naturelles de Bruxelles, Belgium; **NHMUK**, Natural History Museum, London, United Kingdom; **SMNS**, Staatliches Museum für Naturkunde, Stuttgart, Germany.

Anatomical Nomenclature—Osteological anchors (such as scars, ridges, crests) for musculature follow the myological nomenclature of Mook (1921), Iordansky (1973), Meers (2003), Pol (2005), Turner (2006) and Sertich and Groenke (2010).

HISTORICAL BACKGROUND

The discovery of the most complete specimens of the Early Cretaceous goniopholidids was held during excavations for dinosaurs in the Belgian coal mine of Bernissart. Following the first discoveries of dinosaurs in Wealden facies of the "*Cran aux iguanodons*" in the Sainte Barbe pit at Bernissart in 1878, new excavations restarted in May 1879. At this second occasion, a first skeleton (IRSNB R47) was found in the same gallery at a depth of 322 m together with eighteen complete and partial skeletons of *Iguanodon bernissartensis* and two skeletons of the small neosuchian *Bernissartia fagesi*. From this first concentration of fossil vertebrates the gallery was extended for about 50 m in an east-southeast direction across the cran. The second goniopholidid specimen (IRSNB R290) was found on October 22nd 1879 at about 38 m from the entrance of the cran (see Godefroit et al., 2012).

The beautiful specimen IRSNB R47 (Fig. 1) was prepared, mounted in three dimensions and exhibited in the Nassau Palace in Brussels in 1884, next to the first complete skeleton and holotype specimen of *Iguanodon bernissartensis* (IRSNB R51) and the small *Mantellisaurus atherfieldensis* (IRSNB R57). The second specimen of *Goniopholis* IRSNB R290 (Fig. 2) was prepared on one side and left *in situ* in the clay matrix. Today it is exhibited at the Musée de l'Iguanodon in Bernissart.

Both specimens were illustrated in an in situ position by two different artists in 1883 (Fig. 2). IRSNB R47 was drawn by G. Lavalette, famous for other illustrations of *Iguanodon*; IRSNB R290 was drawn by L. Cockelaere.

As for specimens of *Iguanodon*, the age of the goniopholidid specimens is late Barremian to earliest Aptian based on palynological and carbon isotope data of the vertebrate-bearing Wealden facies in Bernissart (Yans et al., 2012).

SYSTEMATIC PALEONTOLOGY

MESOEUCROCODYLIA Whetstone and Whybrow, 1983

COELOGNATHOSUCHIA Martin, Lauprasert, Buffetaut, Liard and Suteethorn, 2014

GONIOPHOLIDIDAE Cope, 1875

ANTEOPHTHALMOSUCHUS Salisbury and Naish, 2011

Type Species—*Anteophthalmosuchus hooleyi* Salisbury and Naish, 2011

Holotype—NHMUK R3876, a partial articulated skeleton from the Vectis Formation of the Isle of Wight, England (Salisbury and Naish, 2011).

Referred Material—IWCMS 2001.446, a partial disarticulated skeleton from the Wessex Formation; IWCMS 2005.127, a partial skull associated to postcranial elements from the Wessex Formation (Salisbury and Naish, 2011); IRSNB R47, a nearly complete mounted skeleton from Bernissart, Belgium (Figures 1–7; 9–20); IRSNB R290, an articulated skeleton missing the skull and mandible. This specimen is still partly encased in the sediment (Figures 2, 8).

Revised Diagnosis—Updated from Salisbury and Naish (2011).

Anteophthalmosuchus hooleyi is diagnosed by the following autapomorphies: orbital portion of lacrimal, prefrontal, frontal capped by a thin, rectangular palpebral; rostrolateral part of postorbital forms a distinct, laterally bowed process that projects from the cranial table partly to encircle the orbit laterally, extending rostroventrally towards, but not quite contacting the dorsal surface of the jugal arch; dorsal outline of supratemporal foramen subcircular and almost twice the maximum diameter of orbits; pterygoid-palatine suture rises acutely from the posterior end of the suborbital fenestra (not visible in IRSNB R47). In addition *A. hooleyi* possesses the following combination of characters: entire cranial table, infratemporal region (excluding the medial surface of the quadratojugal) and the entire maxillary rostrum uniformly covered in similar sized, regularly spaced, roughly circular pits; interorbital transverse ridge absent; absence of antorbital fenestra; lacrimal and rostral part of jugal with distinct shallow groove extending rostrally from the orbital border; palatines with subparallel lateral borders, bulging laterally slightly mid-way along the suborbital fenestrae; internal septum that divides the secondary choanae formed by the pterygoids, extending rostrally to contact the posteriormost extent of the palatines (not visible in IRSNB R47); external mandibular fenestra absent.

Locality and Horizon—Coal mine of Bernissart, Belgium; latest Barremian- earliest Aptian after Yans et al. (2012).

DESCRIPTION

Skull

As the Bernissart specimens are particularly dark and shiny, Figure 1 and Figures 3-7 have been realized by coating IRSNB R47 with ammonium chloride in order to give a neutral grey color and enhance the contrast and relief. The skull IRSNB R47 is nearly complete, the tip of the rostrum being damaged (Fig. 3). It underwent substantial dorsoventral crushing, resulting in a number of cracks and obscuring some features of the palate. The skull can be described as mesorostrine on the basis of the measurements available in Table 2 although it should be reminded that the skull is missing most of the premaxillae. The orbits are circular and so are the supratemporal fenestrae, which are about one third the diameter of the orbits. The entire dorsal surface of the skull is ornamented with a dense pattern of circular pits. Unlike in *Goniopholis simus*, *G. baryglyphaeus* and *Nannosuchus*, the dorsal surfaces of the lacrimal, prefrontal and frontal do not possess any periorbital or interorbital crests; such crests are also absent in the Hooley's specimen (NHMUK R3876) and Hulke specimen (BMNHB 001876) (Andrade and Hornung, 2011).

Premaxilla—The premaxillae are not preserved with the exception of the posterior most region of the left element that still hosts the last alveolus and its tooth. This is supported by the presence of a diastema on the left side corresponding to the embayment between the premaxilla and maxilla. The suture with the nasal or maxilla is not visible due to bone being crushed in this area. Nevertheless, on the dorsal

surface, the preserved portion of the left premaxilla does not show evidence of an external narial fossa. It is therefore assumed that the narial fossa was entirely encircled by the premaxillae and the nasal excluded from its posterior border. The deep embayment visible on the left side at the premaxillary-maxillary junction should have been much more developed when the premaxilla was complete, because the premaxilla in goniopholidids is transversely broader than the maxilla.

Maxilla—The maxillae are complete. In dorsal view, they are slightly inflated laterally at the level of the enlarged caniniform tooth (the fourth) and remain straight posterior to it. Thus in lateral view, the tooth row has a single modest wave with a convex margin at the level of the enlarged caniniform tooth. The rest of the tooth row is straight. The maxilla hosts a large and deep depression on its posterodorsalmost corner. The general outline of this depression is best preserved on the right side and is clearly longer than wide. However, the left depression offers some information on its deepest surface, which seems to be divided dorsally in three smaller concave units. The depression lies almost entirely on the maxilla but dorsally, the depression seems to extend as well onto the contact with the jugal (posterodorsally) and lacrimal (anterodorsally). The suture of the maxilla with the jugal and lacrimal is situated in the dorsal area of the depression (Fig. 4). No antorbital foramen could be detected, and although the skull is poorly preserved in that area, its absence in NHMUK R3876 renders its presence unlikely in *Anteophthalmosuchus*. The ventral side of the maxilla is heavily crushed and an attempt of the maxillary alveolar count is given here. Most alveolar collars are fragmented and in some cases, their position can only be guessed at thanks to the presence of teeth in position. The left tooth row shows the first 13 alveoli, most with teeth in them. From this point, three small alveoli are tentatively

identified and more may have been present but are not recognized. The right toothrow is better preserved and although the first maxillary alveolus is absent, it is possible to give a precise count by comparison of the anteriormost left tooth row with the right tooth row. Therefore, a total of 19 tooth positions can be counted. The fourth alveolus is the largest, as best seen from the right tooth row. From there the alveoli decrease progressively in diameter. The suborbital fenestra is bordered by alveoli 14 to 19. The relationship of the posteriormost region of the toothrow with the right ectopterygoid is unclear because the ectopterygoid is disconnected, but there is no evidence for its participation in the toothrow on the left side because the anterior end of the ectopterygoid is not long enough. The maxilla does not send a process between the toothrow and the ectopterygoid either. The maxilla forms to the anterolateral margin of the suborbital fenestra.

Nasal—The nasal is a long paired bone. Its contacts with the maxilla are mostly detectable but the anteriormost relation with the premaxilla is unclear. The nasal is interpreted as stopping before the level of the premaxillary-maxillary diastema because in the anterior portion of the rostrum the external margins of both nasals converge. Posteriorly, the nasal suture with the frontal is wide and asymmetric due to deformation. Despite such preservation, the frontal splits the nasals posteriorly as in NHMUK R3876. Posterolaterally, the nasal configuration contacts the prefrontal and the lacrimal. On the right element, a thin posterior process is pinched between the lacrimal and frontal. Although affected by deformation, a comparable but transversely broader process is visible on the left side.

Palpebral—A palpebral is preserved as in the Hooley's specimen (NHMUK R3876), Willet's specimen (BMNHB 001876), *Nannosuchus* (NHMUK 48217), and *Goniopholis simus* (IPB R359) (Andrade and Hornung, 2011). The palpebral is sutured to the medial margin of the orbital rim. The best preserved palpebral is the left one. It consists of a curved and anteroposteriorly elongate bone as in the Hooley's specimen (NHMUK R3876). As a comparison, this bone is triangular in outline in the other goniopholidids examined by Andrade and Hornung (2011). In the right orbit, it is disconnected and lower relative to its original position, which can be observed in the left orbit. The palpebral sutures with the frontal posteriorly, with the prefrontal medially and with a knob-like process of the lacrimal anteriorly.

Prefrontal—The prefrontal is best observed on the right side. The palpebral prevents the prefrontal from contributing to the medial border of the orbit. It is teardrop-shaped and longer than wide. It sutures anterolaterally with the lacrimal, anteromedially with the posterior process of the nasal and medially and posteriorly with the frontal. Although heavily crushed, the ventral surface of the left prefrontal shows that the dorsal termination of the prefrontal pillar forms a ridge. This ridge is prominent, curved and it probably extends laterally to the lacrimal. Anterior to this ridge there is a distinct ovoid depression on the ventral surface of the prefrontal. The prefrontal does not meet the postorbital (see Andrade and Hornung, 2011 for an update of this morphology in *Goniopholis simus* and *G. baryglyphaeus*).

Lacrimal—The lacrimal forms the anterior margin of the orbit. It is trapezoidal in outline with its anterior end overlying the maxilla. There is no evidence of an antorbital foramen but the preservation renders fine details difficult to discern, so it is

not possible to fully discard its presence. On the orbital margin, the suture with the jugal is clearly visible and is located in the anterior portion of the orbit, thus the jugal contributes substantially to this area. From the anterior orbital margin, the edge immediately adjacent to the orbit consists of a triangular concave area devoid of ornamentation, smoothly continuous inside the orbit and referred as the lacrimal anterior groove (Fig. 3). Laterally, this groove spreads on the jugal, just above the maxillary depression. The lacrimal contacts the nasal medially. Anterolaterally, it shares a thin contact with the maxilla just above the maxillary depression, but does not take part in it.

Jugal—The jugal is a long bone that contributes to the ventrolateral margin of the orbit and continues far posteriorly, participating in the ventral margin of the infratemporal fenestra. In its anteriormost portion, it consists of an ornamented bulge forming the anteroventral margin of the orbit. In lateral view, the ventrolateral edge of the orbit has an S outline, with the anteriormost region of the jugal distinctly raised dorsally above theposteriormost corner of the maxilla (Fig. 4A, B). Behind the anterior bulge, the jugal slopes ventrally and the smooth internal surface becomes visible dorsolaterally for the rest of the length. Here, this surface presents a shallow keel. The distal ramus of the jugal is subcircular in cross section. The posteriormost extension of the jugal, which is on the lateral edge, stops approximately one centimeter behind the posterior end of the infratemporal fenestra. The quadratojugal/jugal suture is oblique, such that the quadratojugal forms the posterior corner of the infratemporal fenestra (Fig. 3).

Postorbital bar—This area is crushed but some indications are available on the left side. The jugal has a smooth dorsal area, where the postorbital bar originates, just posterior to the orbit. Here, the lateral surface of the bar is smooth, slightly concave and flush with the lateral surface of the jugal (not inset unlike in eusuchians and in some non-eusuchians such as *Eutretauranosuchus* [Smith et al., 2010; Pritchard et al., 2013] or *Paralligator* [Turner, 2015 and JEM, pers. obs.]). The bar, at mid height, is not cylindrical but is strongly mediolaterally compressed and anteroposteriorly elongate. Any relation to the infratemporal corner is hidden by the skull table collapse. The postorbital-jugal suture is visible just below an anteroposterior ridge marking the lateral surface of the bar.

Postorbital—Both postorbitals are complete, but are fractured and displaced in a similar fashion with the anterolateral process of the postorbital pressed against the ventral orbital margin. The squamosal-postorbital suture on the skull table is also affected by a crack. Uniquely among neosuchians, the postorbital contributes to the posterior end in the posterolateral corner of the orbit by means of a long, pointed and anteromedially curved process, much longer than seen in any dyrosaurid, pholidosaurid or *Gavialis*. The anterolateral margin of the skull table therefore possesses a pointed anterolateral projection, which is an extension of the skull table, bearing circular pits on its proximal area. In dorsal view, the medial margin of this extension is concave whereas its lateral margin is anteroposteriorly straight. The lateral surface of the postorbital process is smooth, concave and wide and is ventrally flanked by a longitudinal scar (Fig. 4A, B). This smooth area continues posteriorly as a thin groove on the lateral surface of the postorbital and also of the squamosal. Assuming that the fracture on the dorsal temporal bar developed along the suture

between the postorbital and the squamosal, it can be tentatively stated that the contribution of the postorbital to that bar is less than that of the squamosal.

Frontal—The frontal occupies most of the interorbital area and forms the posteromedial corner of the orbit. Although preservation is unclear, the frontal seems to contribute to the anteromedial corner of the supratemporal fenestra. Contrary to *Eutretauranosuchus delfsi*, *Amphicotylus lucasii* (Pritchard et al., 2013) or species of *Goniopholis* (Andrade and Hornung, 2011), a transverse interorbital ridge is absent and the frontal is completely flat. The frontoparietal suture is visible and occurs between the supratemporal fenestra, about one centimeter behind their anterior margin.

Parietal—The suture with the squamosal seems visible on the left side. The dorsal surface of the parietal is flat, being twice as wide posteriorly than in the interfenestral area. The anteromedial corner of the supratemporal fenestra is facing dorsally. The orbitotemporal foramina are totally obscured due to preservation. The skull table ornamentation is even with the rim of the supratemporal fenestra.

Squamosal—The squamosal prongs are well pronounced, rounded at their distal ends, slightly inflated apically and devoid of any ornamentation. The smooth surface is about two centimeters in transverse width at the base. The prongs taper far posteriorly, well beyond the posterior margin of the skull table. In posterior view, the posterior margin of the squamosal and parietal substantially overhangs the occipital margin of the skull. On the occipital surface, just below the squamosal prong, there is

a small depression, delimited medially by the exoccipital and best seen on the right side of the skull (Fig. 6).

Supraoccipital—The supraoccipital is not discernible from the parietal both in dorsal and in posterior view. Its extent on the dorsal surface of the skull table is unclear even if some fractures could potentially correspond to sutures.

Quadratojugal—The quadratojugal contributes to the posterior margin of the infratemporal fenestra, where it sends a long spine (Fig. 3). Visible on the right side, this intact spine is dorsoventrally flattened and reaches nearly half of the infratemporal length. Mediolaterally, the quadratojugal can be divided in two areas. Laterally, along the lower margin of the infratemporal fenestra, it is ornamented with deep cupules; medially, it is beveled and makes a continuous smooth area from the tip of the spine to its posterior end. This smooth area is continuous with the dorsal smooth surface of the quadrate. The organization of the bone with the otic area or with the postorbital cannot be assessed due to crushing. Ventrally, as seen on the right quadratojugal, a short anterior process projects on the ventromedial side of the jugal infratemporal bar, a centimeter from the posterior tip of the infratemporal fenestra (Fig. 5). The quadratojugal reaches the posterior level of the quadrate condyle and in posterior view, gives the impression of a distinct knob lateral to the quadrate condyle.

Quadrate—The contribution of the quadrate to the braincase is impossible to assess. However, both quadrate branches leading to the condyles are clearly visible. The dorsolateral surface is smooth and slightly concave. Medially, the surface dorsal surface slopes steeply but there is no crest dividing these two continuous zone. As

seen on the left side, the cranioquadrate groove opens posteroventrally, in a similar location as in derived eusuchians. It is pinched ventrally by the paroccipital process and is floored by the medial portion of the quadrate branch. However, unlike derived eusuchians, it is open laterally and although crushing has distorted the quadrate branch upward, the laterally opened cranioquadrate groove is clearly identified (Fig. 6). This groove connects to the otic area, which is covered by sediment on both sides of the skull. Ventrally, the right quadrate preserves a marked crest (crest B of Iordansky, 1973) that runs away from, but almost parallel to the suture with the quadratojugal. This crest is situated anteriorly, far from the condyles, its medial edge being perpendicular to the quadrate surface (0.5 mm high). The quadrate condyles are well preserved although no evidence for a foramen aëreum could be detected. In posterior view, the medial hemicondyle is dorsoventrally high but mediolaterally compressed whereas the lateral hemicondyle is mediolaterally longer (Fig. 6). Thus in outline, the medial one is ventrally pendulous and the dorsal surface between the two condyles is grooved. An evident concavity separates the convex surface of the medial and lateral condyles.

Exoccipital—The exoccipital is only visible in posterior view, although due to crushing it is somehow detectable in dorsal view also. The paroccipital area forms a large plate; its posteroventral edge is rather thick and distinctly convex, and it is grooved in continuity with the cranioquadrate passage. The paroccipital area is smooth and devoid of any boss. Medially, the exoccipital forms the dorsal margin of the foramen magnum and descends as two pillars on the basioccipital condyle. The relationship with the basioccipital is unclear except that on the right side. The hypoglossal foramen is circular and opens just lateral to the foramen magnum. More

laterally and ventrally, two foramina open at the level of the occipital condyle with first a small foramen that could correspond to the vagal foramen vagus, then a larger foramen more laterally that could correspond to the posterior carotid foramen (Fig. 6).

Basioccipital—The occipital condyle is large. Ventrally, the basioccipital plate is short and wide and has the particularity of having strongly recurved wing-like tubera, projecting posteriorly ventrolateral to the condyle. Thus the basioccipital plate does not face posteroventrally but consists of a deeply concave surface, which faces posteriorly and possesses laminar lateral edges (Fig. 6).

Basisphenoid—The basisphenoid is mostly destroyed but its posteroventral portion is still preserved and visible in ventral view between the pterygoid and the basioccipital. Here, the basisphenoid has a concave surface that spreads posteriorly on the basioccipital (Fig. 5) connecting as a wide groove the basioccipital plate to the presently damaged median Eustachian foramen. Although the lateral areas are eroded, they show that the basisphenoid appears ventrally between the basioccipital and pterygoid for about half a millimeter. More distally, a triangular incision separates the posteromedial tip of the pterygoid from the posteriorly pointed lateral edge of the basioccipital described above. Therefore, the basioccipital and pterygoid are not in contact.

Pterygoid—The ventral surface of the skull is heavily crushed making details of the pterygoid difficult to discern. The clearest area is the right one. Here, the pterygoid participates in the posterior margin of the suborbital fenestra, which is wide and straight, clearly separating the palatine from the ectopterygoid. It is presently unclear

whether the pterygoid takes part or not in the palatine bar. The posterior margin of the pterygoid plate is uneven: medially and as described above, a triangular incision separates the pterygoid from the basioccipital projection, then moving laterally, the medial margin of the pterygoid shows a short triangular process, which protrudes further posteriorly than the remainder of the pterygoid margin. This latter portion is wider with its margin mediolaterally expanded (Fig. 5). In ventral view, the lateral margin of the pterygoid wing (= *torus transiliens*) is almost parallel to the lateral margin of the skull. The torus slightly protrudes ventrally at the posterolateral corner of the wing. Laterally, it is flat and with a rugose surface where foramina occur. Dorsally, the wing is concave. The choanae are displaced and crushed, but they are likely opening in the anterior area of the pterygoid. The septum is not visible due to preservation.

Ectopterygoid—Both ectopterygoids are visible in ventral view. The ectopterygoid consists of an elongated plate with a slight ventrolateral torsion. The ectopterygoid supports the ventral margin of the pterygoid and terminates posteriorly as a pointed process that does not reach the posterior margin of the pterygoid wing. Anteriorly along its lateral margin, just before the suture with the maxilla, the ectopterygoid has a concave embayment. Its entire medial margin sends a thin crest into the suborbital fenestra, imparting a marked concavity to that area of the fenestra. Anteriorly, the ectopterygoid becomes wider and thicker in its sutural area. Here, and although poorly preserved, the ectopterygoid does not seem to reach the maxilla but sutures to the jugal only. The ectopterygoid contribution to the suborbital fenestra is about as long as that of the maxilla.

Palatine—The palatine is extensive, making most of the interfenestral length. Posteriorly, it contributes to the anterior margin of the choanae, which open more than five centimeters into the palatine from the posterior level of the suborbital fenestra. The palatine therefore also contributes to a substantial length to the lateral margin of the choanae, but anteriorly it is unclear if the first two centimeters of the interfenestral area are made of the pterygoid or of the palatine. The internal morphology of the choanae cannot be described due to poor preservation. Anteriorly, the palatine seems to project ahead of the suborbital fenestra but the actual reach is only tentatively estimated, as numerous cracks and displacement of bones of the palate render the identification of the maxilla-palatine suture impossible to assess.

Laterosphenoid—The laterosphenoid is best visible on the left side in ventral view. It forms all the anteromedial base of the supratemporal fenestra. The capitate process is thin and although its anteriormost margin is eroded, it is transversely expanded to reach the postorbital. The lateral margin of the bone consists of a thin crest that runs for the entire length of the bone as in *Eutretauranosuchus delfsi* (Pritchard et al., 2013). Posteriorly, the morphology remains unclear because the dorsal surface of the skull interpenetrates with the palate due to crushing.

Mandible

In lateral view, the profile of the mandible is linear (Fig. 7). Although the first dentary alveoli are not preserved, it is expected that a single wave or lateral festooning of the jaw occurs at the anteriormost end. As seen from a medial view, the glenoid fossa on the articular is located approximately at the same level as the toothrow. The pattern of

ornamentation varies, with light furrows in the anterior portion, mainly on the ventral and lateral surfaces of the dentary, whereas on the external surface of the angular and surangular is a pattern of large cupules, similar to those found on the dorsal skull surface and osteoderms. There is no external mandibular fenestra. The left mandible is not crushed and fully confirms this morphology.

Dentary—The anterior portion of the toothrow underwent some damage so it is not possible to give a precise count of the number of alveoli on each dentary. Nine teeth are visible on the right, their lateral alveolar collar also visible. Here, the alveoli gradually decrease in size toward the posterior end. However, anteriorly, alveoli are completely destroyed. A large tooth is still in place but its base has been reconstructed with plaster. The posterior tooth row is completely crushed. On the left side, four alveoli with teeth are visible in the middle of the tooth row, then a large eroded dentary groove hosts at least one tooth root but it is not possible to give any alveolar count. The dentary symphysis can be partially observed in ventral view. It is short, reaching the level of the largest dentary tooth, which corresponds to the third or fourth.

Splenial—The suture of the splenial with the dentary is best seen in ventral view. The splenial tapers far anteriorly, but whether it participates in the symphysis or not is uncertain due to preservation. If the splenial did not participate, it should have approached the dentary symphysis very closely. No evidence for the intermandibular foramen could be found. The splenial builds the medial wall of the mandible, except near the posterior tooth row, where the dentary is visible.

Coronoid—The anterior region of the median mandibular fossa is crushed on both mandibles and hides the coronoid. There, it is not possible to discern the relationships of the splenial, dentary or coronoid.

Angular—The ventral portion of the angular is laminar and can be divided in an external surface ornamented with cupules and a smooth concave medial surface. There is no smooth external attachment surface for the posterior pterygoideus muscle, as seen in some eusuchians (e.g. Fig. 8 in Martin et al., 2014). The angular contributes to the lower margin of the median mandibular fossa and extends posteriorly to the posteroventral tip of the retroarticular process. In the median mandibular fossa, the insertion for M. pterygoideus posterior consists of a thin blade. Just below the suture with the articular, the angular possesses a well-developed ridge that eventually becomes a thin blade near the posterior end. Anteriorly, the angular has a thin dorsal process, lateral to the median mandibular fossa.

Surangular—The surangular forms the posterodorsal portion of the mandible and contributes to the lateral wall of the median mandibular fossa. Its anterior part is excluded from the external surface of the mandible by the dentary, whereas it continues dorsally along the posterolateral margin of the tooth row, but this area is crushed on both mandibles (so maybe for a length of 3 or 4 alveoli; a morphological detail best seen on the right mandible). Anterior to the glenoid fossa, the dorsal surface of the surangular is flat for insertion of M. adductor mandibulae externus superficialis and M. adductor mandibulae externus medialis. This area is bordered laterally by a thick outgrowth, or a continuity of the ornamentation. Near the posterior region of the dorsal smooth area, a thin scar is visible and continues in front of the

glenoid fossa (Fig. 7). Posteriorly, the surangular slopes ventrally in the left element and to a lesser extent in the right element, possibly due to deformation but following the morphology of the retroarticular process. In contrast to the lateral surface, which is covered with circular pits, the dorsal margin is unornamented up to the tip of the retroarticular process.

Articular—The articular forms the posterior wall of the medial mandibular fossa. Here, the anterior margin of the articular descending process is blade-like and there is a large space laterally between the articular and the medial wall of the surangular. The articular then contacts the angular near the bottom of the median mandibular fossa, where the blade-like outline of the fossa is made by the angular. Dorsally, the articular contacts the surangular on its lateral side, at the level of the glenoid fossa. This glenoid is divided into medial and lateral subfossae, which are similar in size and proportions to the quadrate hemicondyles. The medial fossa is therefore dorsoventrally elongated whereas the lateral fossa is mediolaterally expanded (Fig. 7 of right glenoid). The retroarticular process slopes posteroventrally. The flattened dorsal surface of the retroarticular process is broad, slightly concave and medially expanded, with a markedly convex medial edge. The main surface is very thin whereas the posteriormost tip is rounded and thick.

Dentition

Few teeth are preserved and most of the others are heavily damaged. The best example is the large caniniform from the right dentary, which is circular in cross section, with a pointed and slightly recurved apex. As in eusuchians, mesial and distal carinae are observed, dividing a labial convex surface from a straighter but still

convex lingual surface. Approximately nine vertical, fines ridges ornament the labial surface whereas 11 fine ridges ornament the lingual surface. All tooth crowns have this same pattern of vertical ridges on the enamel surface. The best-preserved tooth is the enlarged right maxillary tooth, which shows at least 14 fine ridges on the labial surface of the crown versus 16 ridges on the lingual surface.

Postcranial skeleton

The postcranial skeleton is available in two specimens. One of them (IRSNB R290) consists of a completely articulated postcranium without cranial elements (Fig. 8), on display at the Museum of Bernissart. All postcranial elements of IRSNB R290 are consistent with the elements of IRSNB R47. Because postcranial elements have been completely freed from the matrix in IRSNB R47 (see Fig. 1 for a general view), the description below focuses on this specimen.

Vertebrae

Apart from the atlas-axis complex, a total of 47 vertebrae are preserved including seven cervicals, 15 thoracic, two sacrals, and 23 caudals. The degree of fusion between neural arches and centra is impossible to assess due to poor preservation. All vertebrae are amphicoelous.

Proatlas—The proatlas is complete (Fig. 9A–D). In dorsal view, it has a triangular outline with a low median crest extending along its entire surface. The lateral margins of the bone are nearly parallel to each other and are long and terminate posteriorly as

a spiny projection, which contacts the dorsal anterior surface of the atlas neural arches.

Atlas—The intercentrum is connected to both atlantal neural arches (Fig. 9E–I). The bone is wedge-shaped in lateral view, exhibiting on its posteroventral corner a dorsoventrally expanded facet for the first atlantal rib. In ventral view, the atlas has a deep median excavation. In lateral view, the anterior notch of the neural arch is not excavated and thus barely detectable.

Axis—The odontoid is fused to the axis (Fig. 9J–M). At the base of the neural canal, it has a small pointed anterior process. In lateral view, the anterior margin is laterally inflated just ventral to the contact with the atlas neural arch. Below, the odontoid receives the second atlantal rib. The ventral margin of the odontoid is eroded. The axis is the longest cervical vertebra. Its ventral margin is deeply concave and the centrum is mediolaterally compressed. A short knob corresponding to the hypapophysis is present at the anteriormost ventral margin of the axis centrum. The anterior ventral margin is located about one half centimeter more dorsally than the posterior ventral margin of the centrum. The posterior surface of the centrum is deeply concave. The neural arch is incomplete. The neural spine is only preserved anteriorly and consists of a dorsally oriented blade. The postzygapophyses are in line with the posterior margin of the centrum.

Atlantal and axial ribs—Both the described ribs are from the right side, which is best preserved. The atlantal rib is the largest with a large and thick proximal facet (Fig. 9P, Q). This bone is mediolaterally flat with a blade-like dorsal margin. The

axial rib is complete and twice shorter than the atlantal rib (Fig. 9N, O). Its dorsal lamina is flattened and has a process that is partly broken. The proximal face is dorsoventrally high and the ventral margin convex.

Cervical vertebrae—Seven cervical vertebrae are present (e.g. Fig. 10A, B). All are amphicoelous and with the exception of the heavily damaged second, all possess a concave ventral margin with a hypapophysis located near the anterior edge. The hypapophysis is a small knob that projects below the surface of the centrum and does not show shape variation across the cervical vertebrae. The first, and possibly the second vertebra, has its posterior margin located more ventrally than the anterior margin, as in the axis vertebra. The ventral margins of the last last five cervical vertebrae are horizontal. The neural spine in the first vertebra is longer than high with a convex, rugose dorsal blade. Cervicals 3 and 4 have partial neural spines preserved, which is higher than long. The left prezygapophyseal facet of the first cervical is nearly vertical. Dia- and parapophyses are all distinctly separated. The parapophysis is located on the ventrolateral margin of the centrum. Although they are located in the anterior region of the centrum, they are shifted posteriorly from the anterior margin. The parapophysis is long, occupying almost half of the centrum length in cervicals 3 to 7. The diapophysis is shorter but protrudes out as a long descending process. Neural arches are present but badly preserved.

Cervical ribs—The best example is a right element from cervical 3 (Fig. 10A, B). It has a long posterior process and an anterior process that is only slightly shorter. The dorsal surface is concave, the ventral surface is flat and laminar anteriorly becoming rod-like posteriorly.

Thoracic vertebrae—There are 15 thoracic vertebrae (e.g. Fig. 10C–H). The only complete neural arches are those of the third and tenth thoracic vertebrae. Hypapophyses, consisting of short robust knobs, are visible in the first three thoracic vertebrae. The fourth bears a remnant of a hypapophysis but all other vertebrae are devoid of it, even as these areas are well preserved. All vertebrae are amphicoelous and have a concave ventral surface. Although incipient, the anterior series of thoracic vertebrae shows slightly mediolaterally compressed centra whereas posterior thoracic series shows centra as wide as high. The centrum length also increases progressively from the anterior to the posterior level in the series with the distal ones being proportionally more elongated. The neural spine in thoracic vertebra 3 is short, as long as high, and limited to the posterior level of the centrum with a flat and slightly expanded dorsal margin. In thoracic vertebra 10, the neural spine is longer, occupying most of the centrum length and with a similar morphology as in thoracic vertebra 3. Pre- and postzygapophyses are too fragmentary or non-preserved to be described. Thoracic vertebrae 11–15 are devoid of ribs but possess wide and long transverse processes (unknown for 15). A parapophysis is still visible on the anterior margin of thoracic vertebrae 1 and 2 (at mid-height). This changes in thoracic vertebra 3 (ribs incomplete but seem more aligned facets) where the parapophysis is located ventrally on the medial half of the transverse process. Thoracic vertebrae 4 to 10 have the parapophysis on the anterior margin of the transverse process, which is medially located and becomes positioned laterally according to the posterior position of the vertebrae. The transverse process is rod like and short in the first 3 vertebrae, and then becomes more laterally expanded and more flat when moving posteriorly.

Thoracic ribs—The first ten vertebrae are associated with ribs. The shape of the ribs follows the position of the dia- and parapophyses. Thus the capitulum and tuberculum are separated from each other on two proximal extensive branches at least on the first four vertebrae. Moving posteriorly they become aligned in the same plane with the tuberculum tapering further medially than the capitulum, a situation that tends to be less and less accentuated on posterior ribs (Fig. 10L, M). The anterior margin of the proximal shaft hosts a pronounced blade, which progressively shifts distally. This blade is almost non-existent in the tenth rib.

Sacrum—Two sacral vertebrae are present and still fused to the ilia (Fig. 10I, J). Their neural arch is eroded. The ventral margin of the centrum is markedly concave. The first sacral vertebra shows the best-preserved transverse process contacting the ilia in anterior view. The sacral rib is arched, fused to the ilium and the least deformed side is the right, its distal end is at the same level as the dorsal margin of the centrum. Sacral ribs are more robust (anteroposteriorly elongate) in the second vertebra than in the first. The anterior surface of the first sacral is eroded marginally but the surface is flat. The posterior surface of the second sacral is concave and circular. In ventral view, the first sacral vertebra appears wider anteriorly where it contacts the rib than in its posterior portion.

Caudal vertebrae—There are twenty preserved vertebrae, but a few more may have been present (Fig. 10I, J, K). Until the fifth caudal, the posterior and anterior centrum surfaces are still slightly amphicoelous and circular in outline. Behind, the fifth caudal, all centra are flat with a rectangular outline, being mediolaterally compressed. All centra have a demarcated concave ventral margin. In ventral view, the surface

hosts two longitudinal shallow crests. The centra become more elongated relative to their height from anterior to posterior positions. The neural spine is preserved in vertebrae 4, 7, 8, 9, 10, 19, 20, and 21. It is tall in the first but becomes much shorter in the succeeding vertebrae, being restricted to the posterior region. From a dorsal or ventral view, transverse processes are posteriorly directed with a triangular outline. No evidence of a transverse process could be found behind the 13th caudal due to heavy damage. Nevertheless, the caudal vertebra 20, which is complete, does not have a transverse process. The posteroventral margin of the centrum has two facets receiving chevrons. A few chevrons are preserved (Fig. 10N, O, P), the most complete is in front of the vertebra 14 and 15. These chevrons do possess a distal anteroposteriorly spatulate end as well as separated proximal facets.

Shoulder girdle

Scapula—Both scapulae are preserved. The right one is more complete, although still missing part of the blade on the anterior edge (Fig. 11A–D). This bone consists of a dorsally narrow and proximodistally elongate blade. The blade shows a slight anteroposterior constriction where it merges with the proximal portion of the bone. In lateral view, the scapular blade is not perpendicular, but is oblique to the synchondrosis for the coracoid. A small crest for M. triceps brachii sits on the posterior edge of the blade, dorsal to the glenoid process. Visible medially or anteriorly, the deltoid musculature leaves a thin and curved crest. Lateral to it, the acromion process is visible but not distinctly expressed and is located at the anterior edge of the proximal portion of the scapula.

Coracoid—The shape of the coracoid is very similar to that of eusuchians in presenting a pendulous contribution for the glenoid facet on its posterior side and a long ventral shaft expanding at the mid-point becoming a fan-shaped blade with a convex edge (Fig. 11E–H). In lateral or medial view, the coracoid blade is not perfectly symmetrical, the anterior edge has a pointed process. The anterior edge of the blade is markedly concave whereas the posterior edge is straight to convex. An inward curvature characterizes the blade in anterior view. The circular coracoid foramen is close to the glenoid. The coracoid forms more of the glenoid facet than the scapula. Following the suture with the scapula, the longest sutural face on the synchondrosis slopes steeply on the posterior portion of the proximal area of the coracoid.

Interclavicle—The interclavicle is preserved (Fig. 11I, J). The dorsal surface of the bone is slightly inflated and mediolaterally expanded at mid-length. The interclavicle bears a set of striations on the posterior half (same side as the inflation).

Forelimb

The humerus (Fig. 12A–D) is 20.8 cm long and is less than a third longer than the radius and ulna (Fig. 13A–I). The ulna is 15.6 cm long; the radius is 13.2 cm long. Distally, the ulna is not in line with the radius and finishes more distally than the radius. This is reflected in the shape of the radiale.

Humerus—Only the right humerus is complete, the left one is preserved only proximally. It consists of a long straight shaft. The deltopectoral crest is a short lamina restricted to the proximal region on the anterolateral margin of the shaft.

Posterior to the deltopectoral crest are two areas of insertion for the M. teres major and M. dorsalis scapulae. A shallow groove is present on the proximal posterior surface, close to the humeral head. The head of the humerus is not developed, although it sits on the proximalmost end of the humerus. On the other hand, the medial humeral process is thicker. Distally, the ulnar hemicondyle tapers slightly further than the radial hemicondyle. A shallow trochlea separates both condyles anteriorly, whereas posteriorly there is a shallow depression that does not extend proximally. On the lateral surface of the ulnar hemicondyle, a small epicondyle is present.

Ulna—Only the right ulna is preserved. It is highly fractured and the distal end is badly preserved and still connected to a bone. The ulna is nearly straight and tubular throughout its length with the proximal part becoming flat and expanded anteroposteriorly. The anterior margin of the proximal part is concave with an overhanging radial facet whereas the posterior margin is convex. The proximal head of the ulna is eroded laterally and some bone is missing on the medial side, just below the olecranon process. This process is proximally marked as a pointed spine on the posterior margin, thus the humeral articular surface is concave and narrow there. More anteriorly, as is visible in proximal view, the rest of the facet for the humerus-ulna articulation is as long as wide and convex. On the medial margin of this articulation, above the radial facet, there is a developed scar, which descends as a crest along the medial side of the shaft, thus delimiting the anterior margin of the pronator quadratus fossa (there is no fossa in *C. niloticus* IRSNB 20.150). Posterior to this fossa, a set of three longitudinal fine grooves corresponds to the medial flexor ridge and ascends to the olecranon process. The distal end of the bone bears a

prominent scar on the anterolateral process, which is pierced anteriorly by a large foramen (2.5 mm in diameter). The anterior surface presents a groove but this is not well preserved. Medially, an even more obvious groove is separated by the anterior and posterior developed oblique processes. On the posterior surface, a shallow groove extends along most of the shaft length.

Radius—Only the right radius is preserved. Its distal facet is damaged. The radius has a straight shaft that is slightly deformed and has been restored. The proximal surface for the humerus is mediolaterally expanded and is concave. In proximal view, the posterior margin is straight and the anterior margin is slightly convex. Medially, the bone projects above the shaft. The distal end is more massive than the rest of the bone, being expanded anteroposteriorly.

Radiale—The radiale (Fig. 14E–H) is an elongated bone (unlike in eusuchians, e.g. Mook, 1921) with a nearly straight but slightly concave medial margin. The lateral edge of the shaft is shorter and more concave. The lateral facet for the ulna is remarkably long (1.6 cm) and hosts a spiny posterior process at its distal edge, serving as a contact with the ulnare. Another more massive posterior process is located at the base of the radial facet, thus the proximal posterior surface of the shaft is deeply concave. The distal end of the bone expands mediolaterally, being teardrop shaped in distal view with a thin lateral expansion contacting the ulnare.

Ulnare—The proximal end of the ulnare (Fig. 14A–D) is as wide as the shaft and the distal end of the bone is fan-shape, thus the medial and lateral margins are widely concave. Laterally, just before mid-shaft, there is a small anterolateral scar. The

distomedial facet contacting the radiale consists of a short peg. Proximally, the facet is rounded and convex. The distal facet is eroded.

Manus—**(**Fig. 14I–V**).** The right manus shows five digits and, although all metacarpals are preserved, only digits I, II and V preserve phalanges. In digit I, the first phalanx is short and relatively robust, whereas in digit II, the first phalanx is gracile and about twice as long as the same phalanx in digit I. Metacarpal III is the longest of all but is only slightly longer than metacarpals II and IV. Metacarpal III possesses a globular callosity on its proximal head. The proximal region of metacarpals II and V are anteroposteriorly flattened. Metacarpals I and V are about twice as short as other metacarpals. Metacarpal I possesses wide and thick proximal and distal articular surfaces.

Pelvic girdle

All the elements of the pelvis are present. The bones have been deformed in some places, but retain their general shape. Some parts have been restored, especially along fractures. Bones from the pelvis are similar to that of other mesoeucrocodylians when they have been described. Minor differences are highlighted.

Ilium—Both ilia are incompletely preserved and variably affected by plastic deformation. The right one is heavily fractured, but the left one is not (Fig. 15). The dorsal margin of the blade is convex, has a low profile and is moderately wasp-waisted posteriorly, as seen on the right element. This feature is barely detectable on the left ilium. Although a set of fractures have been filled with plaster on the lateral side, the dorsal margin and the medial side are not damaged, fully connected and

therefore the general morphology is congruent with the original. A spiny process of the ilium is present; it is anteriorly projecting, and overhangs the concave anterior margin of the supraacetabular crest. The posterior process is as long as the acetabulum area and terminates with a deep blade (for comparison see Brochu [1999, fig. 29]). This is not visible on the left element due to deformation and breakage of the posteriormost tip.

The supraacetabular crest is restricted to the anterodorsal margin of the acetabulum (as in *C. niloticus*). Its shape is best preserved on the left ilium. Two anteroventral peduncles connect to the ischium and form the anterior and posterior margins of the hollow acetabulum, respectively (Fig. 15A). In ventral view, the anterior peduncle has a triangular outline. The posterior peduncle is mediolaterally enlarged and has the shape of a half moon. The medial surface of the ilium is only visible dorsally on the left element. It is smooth and slightly concave just below the rugose dorsal margin.

Ischium—Both ischia are preserved although the left more completely preserves the articular facets (Fig. 15B–E). The proximal area is anterolaterally expanded and is divided into two facets that articulate with the ilium. In proximal view, the anterior and posterior iliac processes are not aligned with the anteroposterior axis of the ischial blade. These two processes are separated by a marked notch corresponding to the acetabulum, which is flush with the medial margin of the ischial shaft and is demarcated by a ridge on the lateral margin of the shaft. The anterior iliac process is divided into a medial and a lateral ilial facet. The surface of the pubic facet is flat and protrudes distinctly in an anterior direction as a transversely ovoid process separated from the dorsal surface of the anterior ilial process. Dorsally, the facet of the anterior

ilial process is concave, anterolaterally directed and longer than wide. The posterior ilial process is robust and ovoid in cross section and hosts two articular facets of comparable size in dorsal view. The dorsomedial facet accommodates the ilium and the dorsolateral facet consists of the posterior margin of the acetabulum.

The ischium is wasp-waisted at mid-shaft and the anterior margin is thin in comparison to the posterior margin. The medial surface of the shaft is flat whereas an oblique crest extends on the lateral surface from the lateral edge of the anterior iliac process onto the posterodorsal margin of the distal blade. The ventral, or distal, margin of the blade is anterolaterally expanded, being wider than the proximal area of the bone. The ventralmost margin is damaged. This blade curves medioventrally, so that its internal surface is slightly concave.

Pubis—Both pubes are complete (Fig. 15F) but the anteromedial margin of the right is damaged. The bone is flattened throughout. The proximal facet for the ischium is ovoid, being wider than tall. In dorsal view, its proximal area is depressed. The distal blade is spatulated with a wing-shaped end that expands rapidly after the constriction of the proximal portion of the shaft. The blade is slightly concave on its ventral surface. The medial margin is strongly concave; the lateral margin is convex and is thick throughout its length. In dorsal or ventral views, the outline of the distal margin of the pubis is concave and beveled toward the medial margin.

Hind limb

The femur is about one third longer than the tibia and fibula (Figs. 16, 17). The femur has a proximodistal length of 20.1 cm, the tibia of 14.4 cm and the fibula of 13.8 cm.

Femur—Both femora are preserved and complete. The femur has a sigmoid shaft in lateral view and resembles the femur of *Bernissartia fagesii* (IRSNB R46) and other derived neosuchians. The proximal head of the femur is mediolaterally flattened and bears on its lateral surface a shallow concave area, and on its posteromedial side, a knob-like process (Fig. 16B,C). Contrary to the great trochanter, the fourth trochanter is well developed and is visible in medial and posterior views. Dorsal to the fourth trochanter, a large and slightly concave insertion area for the caudofemoralis muscle is visible. Distal to the fourth trochanter, a thin scar corresponds to the primary adductor attachment. Distally, the condyles for tibia and fibula are individualized, of comparable dimension and are nearly aligned with each other. On the anterior surface, the intercondylar groove is visible but remains shallow and restricted to the distalmost area of the femur. On the posterior surface, both condyles are separated by a deep popliteal fossa (Fig. 16C).

Tibia—The tibia is a long straight bone with moderately expanded distal and proximal ends. The anterior margin of the shaft is rounded and the posterior margin is flat. Near both the proximal and distal ends , facets are visible on the posterolateral margins of the tibia to accommodate the fibula (Fig. 17B, C).

Fibula—The fibula is a slender and straight bone, more or less circular in cross section to the exception of the flattened proximal end, which curves posteriorly. Near the proximal end of the bone, the flat medial surface comes in close contact on a lateral facet of the tibia. The iliofibularis trochanter is visible as an ovoid scar on the anterolateral margin of the fibula, at the base of the proximal curvature of the bone.

The distal end of the fibula is anteroposteriorly elongated and its medial surface contacts the distal end of the tibia.

Astragalus and calcaneum—These two bones (Fig. 18) are much similar to those of eusuchians in shape and proportions (e.g. *C. niloticus* IRSNB 20.150). The right calcaneum is preserved and is pressed against the astragalus and two rounded ossifications that correspond to the distal tarsals. The calcaneum is well visible laterally, showing the outline of the anterior ball and the posterior tuber. These two structures are well separated by a markedly notched area. The astragalar facet, located medially to the anterior ball is not visible because the astragalus is in articulation. The posterior tuber is damaged but a groove is visible. The ventral surface of the anterior ball (or distal tarsal facet) is flat whereas on its dorsal surface the ball is convex. Laterally, the margin of the ball possesses is thick and the main lateral surface is flat, hosting a short proximodistal crest. The astragalus is mediolaterally expanded, possessing a large rounded medial head. The tibial facet is concave and divided in a dorsoventrally expanded area medially and into a shorter rectangular area laterally. In the middle, the astragalar fossa is covered in glue.

Pes—The right pes (Fig. 19) is the better preserved and less deformed than the left one. No phalanges are preserved. Two distal tarsals consist of small rounded bones that connect between the astragalus-calcaneum complex and the proximal articulation of metatarsals I-III. From I to V, all metatarsals overlap each other by projecting a small proximolateral peg on their neighbor. Thus a medial facet is observed on metatarsals II, III and IV. Metatarsal V is shifted laterally and not involved in the overlap and does not show a facet for reception of metatarsal IV. Metatarsal I does

not have a facet either. Metatarsal I is triangular in outline in proximal view whereas metatarsals II, III and IV have a flat mediolaterally expanded proximal head with thick lateral sides. Metatarsals II and III are the longest. The first four metatarsals have long shafts that terminate with a bilobate and symmetrical quadrangular distal articular facet. The dorsal surface of the distal articular facet possesses a short trochlea. Metatarsal I has a distinct scar on the dorsal surface at mid-shaft length. The distal and proximal facets are not in line with the shaft being medioventrally twisted approximately 15°. The shaft of Metatarsal V is greatly reduced, the distal facet is a short pointed process. The proximal facet is however mediolaterally expanded and triangular and concave in proximal view. Laterally, the surface is slightly concave.

Osteoderms

The dermal armor of IRSNB R47 (Fig. 20) consists of a dorsal shield composed of a bilateral row of mediolaterally expanded osteoderms and a ventral shield, composed of polygonal osteoderms sutured to each other. These dorsal and ventral arrangements are typical of the condition in a number of mesoeucrocodylians lineages including Goniopholididae, Pholidosauridae and Thalattosuchia.

Dorsal shield—Twenty-three thoracic osteoderm positions are counted on the left side, and 24 on the right. The osteoderms (Fig. 20) are more or less square in outline anteriorly and progressively become wider in posterior positions. The thoracic osteoderms attain their maximal width near the anteroposterior midpoint of the row (i.e. at the level of the 12th). From this point, the width of the osteoderms becomes progressively narrower moving posteriorly. At any position, the osteoderms preserve a similar anteroposterior length. All osteoderms are roughly flat and ornate with large

circular pits, similar to those seen on the external surface of the skull and mandible. To the exception of the anteriormost osteoderm, which might be incomplete, all dorsal osteoderms possess a forward projecting spine originating from the anterolateral corner (Fig. 20B–D). The spine is not straight but in dorsal view shows an inward curvature. This anterolateral spine inserts below the posterolateral corner of the anteriorly adjacent osteoderm. This spine is completely hidden by the anteriorly placed osteoderm and is therefore invisible in dorsal view. All osteoderms articulate with the anteriorly adjacent osteoderms by an overlap, the anterior osteoderm overlapping the posterior one. The anterior margin of each osteoderm is straight and bears no distinct articular facet for the reception of the anterior osteoderm. On the lateral side of each osteoderm, there is an anteroposterior carina, which is not dorsally elevated but projects above the lateral wall of the osteoderm. In dorsal view, the outline of this carina is convex. In lateral view, each osteoderm is almond shape, the anterolateral spine hidden by the next anterior osteoderm. Circular pits are obvious here. The posterolateral margin of each osteoderm consists of a short pointy spine that projects posterolaterally. In ventral view, the osteoderms are smooth and the articulating anterolateral spine is well visible.

Ventral shield—The ventral shield (Fig. 20E–F) is incompletely preserved in IRSNB R47 and consists of three slabs composed of several polygones sutured to each other. The ventral surface of all these osteoderms is ornamented with deep circular pits and is completely flat, whereas the internal surface is smooth. There is no general orientation of the osteoderms and it is not possible to give a precise position. However, the ventral shield appears to be located around the sternum and possibly near the gastric region, as evidenced by the presence of some disarticulated ribs or

gastralia on the internal surface of some slabs. The individual ventral osteoderms present two morphotypes. In the periphery of the shield, they are trapezoidal with a convex lateral edge. The most medial edges are always sutured to other osteoderms and these osteoderms may have a total of four to five sides. Osteoderms located in the centre of the shield are often hexagonal and are the largest in comparison to the peripheral osteoderms. The hexagonal osteoderms are sutured to all surrounding osteoderms along their entire margins, thus the ventral shield does not show any void between the elements.

Other osteoderms—A small osteoderm is stuck on the proximal portion of the right scapula and another triangular one is stuck on the proximal head of the right humerus. Their presence might be indicative of a limited osteoderm ossification on the appendicular skeleton.

PHYLOGENETIC ANALYSIS

The coding initially established by Andrade et al. (2011) for Dollo's goniopholidid was expanded based on our firsthand revision of the associated specimens and the taxon was subjected to a phylogenetic analysis in the software TNT (version 1.1, Goloboff et al., 2003). A heuristic search of 1000 replicates of Wagner trees using random addition sequences was followed by TBR branch swapping. A final round of TBR branch swapping was performed on the trees stored in memory. This taxon is one of the most complete neosuchian to be coded in a phylogenetic analysis, with the updated coding amounting to 89% of the character list. Out of the dataset of Andrade et al. (2011), all thalattosuchians were removed because of the recent phylogenetic hypothesis that recovers them as basal

crocodylomorphs (Wilberg, 2015) and not as nested within neosuchians if kept in the analysis. A total of 89 taxa were analyzed. As in Martin and Buffetaut (2012), the character about the maxillary depression was revised to have three states (supplementary data), and pholidosaurids were updated accordingly. The new matrix is available in the supplements as well as on Morphobank.

Results. The interrelationships of Goniopholididae with other members of Mesoeucrocodylia will not be commented on, as this is part of an ongoing work by the lead author. The topology obtained within Goniopholididae (Best tree length = 1988; consensus of 4 trees; CI = 0.325; RI = 0.793; Figure 21; supplementary data) is identical to that presented in Andrade et al. (2011). *Anteophthalmosuchus* from Britain and Belgium fall in a sister group position, supporting their attribution to the same taxon. Together with *Hulkepholis*, they form a clade that is in a sister group position to the genus *Goniopholis*. The basalmost goniopholidid is *Calsoyasuchus*, and *Sunosuchus* clusters in a clade with *Eutretauranosuchus*. *Siamosuchus*, *Amphicotylus* and *Nannosuchus* have intermediate positions between the basal members (*Calsoyasuchus* and *Sunosuchus*) and derived members (*Goniopholis*, *Hulkepholis* and *Anteophthalmosuchus*). *Sunosuchus thailandicus* does not belong to the genus *Sunosuchus* and is no longer considered a member of the Goniopholididae (Martin et al. 2014) as it was recently demonstrated to belong to the Pholidosauridae and the generic name *Chalawan* was created for it.

DISCUSSION

Taxonomic referral and phylogenetic perspectives

The taxonomic content of the genus *Goniopholis* was revised by several authors (Salisbury et al., 1999; Salisbury, 2002; Schwarz, 2002; Andrade et al., 2011;

Salisbury and Naish, 2011; Buscalioni et al., 2013). One consequence of such work allows recognizing that European Goniopholididae are composed of four to five genera: *Anteophthalmosuchus*, *Goniopholis*, *Hulkepholis*, *Nannosuchus* and possibly *Vectisuchus*. Although *Nannosuchus* has sometime been viewed as a juvenile form of *Goniopholis* (Salisbury, 2002), recent interpretations seem to recognize this genus as valid (Andrade et al., 2011). Concerning *Vectisuchus*, it was originally viewed as a longirostrine goniopholidid (Buffetaut and Hutt, 1980) and Andrade et al. (2011) recently recovered it as part of the Pholidosauridae. To the exception of a few characters, the Dollo specimens fully comply with the diagnosis of *Anteophthalmosuchus hooleyi* Salisbury and Naish, 2011 from the Wealden of England. The English specimens and the Bernissart specimens all share the following unique combination of characters (see Andrade et al., 2011; Salisbury et al., 2011) for bone ornamentation, absence of transverse interorbital ridge, palatine with subparallel lateral borders that bulge slightly midway along the suborbital fenestrae, absence of external mandibular fenestra. The following characters are observed in IRSNB R47 from Bernissart and confirmed as autapomorphic for *A. hooleyi*: presence of a small palpebral, presence of a groove on jugal/lacrimal anterior to orbits, distinct bowed postorbital encircling the orbit, subcircular supratemporal foramen almost twice the diameter of orbit. Nevertheless, the following characters by Salisbury and Naish (2011) are not considered valid because they could be a consequence of preservation or ontogenetic variability and they have not been seen in the Bernissart specimens: the rostral process of frontal ends in a sharp point. The relative size of the occipital condyle compared with the foramen magnum is not a robust example because the foramen magnum can easily be deformed or affected by ontogenetic change. Moreover, in IRSNB R47 the condition is opposite to that seen in the Wessex

specimens where the occipital condyle is slightly larger than the foramen magnum. The position of the dorsal crest of the ilium relative to the supraacetabular crest in the Wessex specimen was found diagnostic according to Salisbury and Naish (2011). However, the specimen IRSNB R47 shows that the relative positions of this feature are variable when comparing the left and right ilium, as a result of deformation. For this reason, we do not retain this character in the diagnosis. Finally, a number of characters are not preserved in the Bernissart specimens: pterygoidopalatine suture and internal septum are crushed. Nevertheless, there are sufficient characters that support the diagnosis of *A. hooleyi* and we view the specimens from Bernissart as belonging to this species.

Recently, Buscalioni et al. (2013) described new goniopholidid specimens from the Albian of Spain. Besides erecting a new genus, *Hulkepholis*, for *Hulkepholis plotos* from Spain (Buscalioni et a. 2013) and for *Hulkepholis willetti* from England (Salisbury and Naish, 2011), Buscalioni et al. (2013) also recognized the presence of a second species of *Anteophthalmosuchus*, *Anteophthalmosuchus escuchae*. We haven't had the opportunity to compare these specimens with *Anteophthalmosuchus hooleyi*.

Andrade et al. (2011) explored the affinities of European goniopholidids and coded those characters of IRSNB R47 visible through the display glass in the Brussel exhibition. In the present work, updating such coding support the phylogenetic hypothesis of Andrade et al. (2011) as well as earlier interpretations (Salisbury et al., 1999; Salisbury, 2002; Salisbury and Naish, 2011) that the Hooley and Dollo specimens are conspecific and belong to *Anteophthalmosuchus hooleyi*. The emerging picture is the existence in Europe of two goniopholidid lineages (Andrade et al. 2011; Buscalioni et al. 2013): a *Goniopholis* lineage including *Goniopholis baryglyphaeus,*

Goniopholis crassidens, *Goniopholis kiplingi* and *Goniopholis simus*; and another lineage composed of *Anteophthalmosuchus* and *Hulkepholis*. At a wider phylogenetic scale, the placement of Goniopholididae with other neosuchian lineages has not reached a consensus yet and will have to be assessed in future work (e.g. Martin and Buffetaut, 2012; Turner and Sertich, 2013; Turner, 2015). Andrade et al. (2011) recover Goniopholididae in a relatively derived position within Neosuchia. However, it should be noted that such results recover longirostrine lineages (Pholidosauridae, Dyrosauridae, Thalattosuchia) closely related to each other, a phylogenetic hypothesis that is not consensual with other works placing Thalattosuchia at the very base of Crocodylomorpha (e.g. Wilberg, 2015a, 2015b) and reconciling with hypotheses proposed before the advent of cladistics (Buffetaut, 1982). Other recent studies recovered Goniopholididae close to Pholidosauridae (Martin and Buffetaut, 2012) into a clade named Coelognathosuchia (Martin et al., 2014), although the inclusion of Dyrosauridae was not tested in that framework. The presence of a maxillary depression in the posterior region of the skull of both pholidosaurids and goniopholidids gives support to this hypothesis. Certainly, coding skull characters alone leads to problems in long-branch attraction (e.g. the longirostrine cluster of dyrosaurids, pholidosaurids and thalattosuchians discussed above, see also Pol and Gasparini, 2009). The description of postcranial characters in distinct lineages will help in clarifying phylogenetic hypotheses and phylogenetic analyses will have to wait for comprehensive descriptions of the postcranial skeleton of other neosuchians.

Key postcranial features of *Anteophthalmosuchus hooleyi*

Postcranial elements of crocodylomorphs are widely encountered in the fossil record of freshwater deposits and are often found as isolated elements. For this

reason, it is difficult to assign isolated postcranial elements to a particular taxon with the consequence that in many cases only the cranial remains are known. With isolated vertebrae at hand, it is generally difficult to go beyond the procoelous/amphicoelous dichotomy to discuss the presence of non-eusuchians or eusuchians. The present description of two articulated skeletons of *Anteophthalmosuchus hooleyi* offers a rare opportunity to associate cranial elements with a postcranium.

With its sigmoid femur and forelimbs proportionally shorter than hind limbs, the appendicular skeleton of *Anteophthalmosuchus hooleyi* is very similar to that of any extinct or modern semi-aquatic neosuchians. Nevertheless, relevant differences are noted below. The humeral shaft is long and markedly straight as in primitive mesoeucrocodylians such as *Simosuchus clarki* or *Mahajangasuchus insignis*. It is however unlike in some eusuchians such as *Stangerochampsa mccabei* with a marked anteroposterior bend of the shaft (plate 2 in Wu et al., 1996a) or *Crocodylus niloticus*, which has a curved outline both anteroposteriorly and dorsoventrally. However, the proximal head presents a medial bend, a condition not present in *Mahajangasuchus insignis* (plate 3 in Buckley and Brochu, 1999). The scapula of IRSNB R47 possesses the general proportions observed in some derived eusuchian scapulae (e.g. *Crocodylus niloticus* IRSNB 20.150). When compared to Cretaceous derived neosuchians, this shape resembles that of *Isisfordia duncani* (fig. 2 in Salisbury et al. 2006), *Susisuchus anatoceps* (fig. 3 in Salisbury et al., 2003) or *Pachycheilosuchus trinquei* (fig. 6 in Rogers, 2003). The scapula does not resemble that of Thalattosuchia, which is rod-like (e.g. *Steneosaurus*, fig. 41 in Andrews, 1913a). However, the scapula of IRSNB R47 drastically differs from that of basal mesoeucrocodylians, which do possess a relatively short and dorsally wide or fan-shaped scapular blade as seen in some notosuchians including *Simosuchus clarki* (fig.

2 in Sertich and Groenke, 2010) and *Araripesuchus tsangatsangana* (fig. 68 in Turner, 2006); or among Dyrosauridae as *Congosaurus bequaerti* (plate 4 in Jouve and Schwarz, 2004); or also as in *Mahajangasuchus insignis* (plate 2 in Buckley and Brochu, 1999). A similar fan-shaped scapular blade has been reported in some alligatoroids such as *Diplocynodon*, *Stangerochampsa* or *Wannagosuchus* (fig. 51 in Brochu, 1999; plate 2 in Wu et al., 1996; fig. 10 in Buscalioni et al., 2011).

The coracoid morphology is similar to that of eusuchians and is not that different from that of the notosuchian *Simosuchus clarki* (fig. 4 in Sertich and Groenke, 2010) but in this species, the shaft markedly widens near its distal end, not at mid-way. Further differences are noticed with the coracoid of *Araripesuchus tsangatsangana* (fig. 69 in Turner, 2006) and *Congosaurus bequaerti* (plate 4 in Jouve and Schwarz, 2004) in the morphology of the shaft, because in both species, the ventral shaft is narrow with parallel sides and only expands as a convex blade at its distalmost edge. In *Pachycheilosuchus trinquei* (fig. 6 in Rogers, 2003), the coracoid blade appears relatively shorter than in IRSNB R47 and the distal blade is almost not expanded.

The wasp-waisted ischium is widely observed among crocodylomorphs to the exception of the dyrosaurid *Dyrosaurus maghribensis*, which possesses wide and nearly parallel anterior and posterior margins (fig. 17 in Jouve et al., 2006).

The axial skeleton of *Anteophthalmosuchus hooleyi* shows the same count of cervical, thoracic and sacral vertebrae as in other neosuchians. The vertebrae of *Anteophthalmosuchus hooleyi* are amphicoelous with centra slightly longer than tall as is the case in other goniopholidids where vertebrae have been reported (*G. crassidens* Owen 1841; *G. baryglyphaeus* Schwarz, 2002; *Siamosuchus phuphokensis* Lauprasert et al., 2007; *Sunosuchus jungarrensis* Wu et al., 1996b. This general

morphology is widely observed among other non-eusuchians with a semi-aquatic lifestyle such as *Mahajangasuchus insignis* (Buckley and Brochu, 1999), Pholidosauridae (*Sarcosuchus imperator* see Fig. 3 in Sereno et al., 2001); *Terminonaris robusta* see Fig. 5 in Wu et al., 2001), or *Bernissartia fagesii* (Buffetaut, 1975) and for this reason offer little diagnostic value. However, the vertebrae of *A. hooleyi* are not comparable to those of Dyrosauridae, which present extremely tall neural spines and ventrally laminar hypapophyses at the level of the first thoracic vertebrae (Schwarz et al., 2006); nor are they comparable to the vertebrae of thalattosuchians in the orientation of the zygapophyses (Krebs, 1962).

The bipartite organization of the dorsal armour of *A. hooleyi* is typical for non-eusuchians (Salisbury and Frey, 2000; Salisbury et al., 2006). The individual units of the dorsal shield of *A. hooleyi* are characteristic of ceolognathosuchians (see review in Martin, 2015). Dorsal osteoderms wider than long flanked by a spiny anterolateral process are common features of both Goniopholididae (*Goniopholis*, *Sunosuchus jungarrensis*, *Siamosuchus phuphokensis*, *Vectisuchus leptognathus*, plate IV, Owen, 1878; Buffetaut and Hutt, 1980; Wu et al., 1996b; Lauprasert et al., 2007) and Pholidosauridae such as *Pholidosaurus decipiens*, *Sarcosuchus imperator*, and *Oceanosuchus boecensis* (Andrews, 1913b, Sereno et al., 2001; Hua et al., 2007). The dorsal osteoderms with the most resembling morphology are those of Teleosauridae, which are square to rectangular in outline and also possess an anterolateral process (Westphal, 1962). All other semi-aquatic crocodylomorph lineages have no comparable dorsal shield to that of *A. hooleyi*: in Dyrosauridae, the osteoderms are subrectangular (Jouve et al., 2006; Schwarz-Wings et al., 2009) and in *Mahajangasuchus insignis* they are sub-quadrangular or ovate and bear a strong median keel (Buckley and Brochu, 1999). The osteoderms of derived neosuchians are

square-like, bear a median keel and have a tetraserial arrangement (e.g. *Bernissartia fagesii* in Buffetaut, 1975; see also Salisbury and Frey, 2000; Salisbury et al., 2006).

The ventral shield of *A. hooleyi* is composed of numerous polygonal osteoderms. Polygonal osteoderms are sometime recovered as isolated material and have only been positively associated with coelognathosuchians such as *Terminonaris robusta* (Wu et al., 2001), *Pholidosaurus decipiens* (Andrews, 1913b), *Crocodileimus robustus* (Lortet, 1892), *Sunosuchus junggarensis* (Wu et al., 1996b) or *Siamosuchus phuphokensis* (Lauprasert et al., 2007). The ventral shield is extensive in Teleosauridae (Westphal, 1962), but contrary to *A. hooleyi* or other coelognathosuchians mentioned above, individual elements are not all perfectly polygonal.

Due to taphonomic circumstances, postcranial elements are often difficult to associate with cranial elements. Because the great majority of fossil crocodylomorph taxa have been erected on the basis of cranial elements, we are still lacking a clear picture of the variability of postcranial elements across the different lineages. Together with previous studies (e.g. Pol, 2005), we recognize that many elements are difficult to prove helpful in diagnosis, especially when found isolated. Nevertheless, important similarities and differences are noted between lineages.

In conclusion, features of the appendicular skeleton are dissimilar when comparing the goniopholidid *Anteophthalmosuchus* with dyrosaurids and thalattosuchians, whereas other features of the dorsal and ventral shield appear to represent reliable diagnostic features of Coelognathosuchia (see also Martin, 2015). All these elements will have to be included in future broad phylogenetic assessments.

ACKNOWLEDGMENTS

At the Royal Belgian Institute of Natural Sciences, we thank A. Folie, curator of Paleontology collections, and M. Haemelinck, head of Museology survey, for access to the mounted specimen IRSNB R47 and the organisation of the opening of its delicate glass cage. This has been done thanks to the technical staff leaded by M. Planchon who was assisted by S. Berton, H. De Potter, E. Dermience, A. Drèze, P. Kileste, B. Lambert, J.-M. Lefever, D. Lieffenrinckx, L. Trevels, and F. Vanderlinden. We add a special thank you to E. De Bast for realizing pictures of Figure 1 and S. Berton for restoration of parts of the Bernissart skeleton. At Bernissart Township, we thank L. Savignat from the Musée de l'Iguanodon for access to the specimen IRSNB R290. This research was supported by Synthesys Project BE-TAF-2788 (to JEM) funded by European Commission (http://www.synthesys.info/). MD was supported by Università di Torino (Fondi di Ricerca Locale 2012, 2013, 2014) and Generalitat de Catalunya (2014 SGR 416 GRC). The last version of this work benefited from the comments of one anonymous reviewer and Marco Brandalise de Andrade as well as the editor, Alan Turner.

LITERATURE CITED

Andrade, M. B., and J. J. Hornung. 2011. A new look into the periorbital morphology of *Goniopholis* (Mesoeucrocodylia: Neosuchia) and related forms. Journal of Vertebrate Paleontology 31: 352–368.

Andrade, M. B., R. Edmonds, M. J. Benton, and R. Schouten. 2011. A new Berriasian species of *Goniopholis* (Mesoeucrocodylia, Neosuchia) from England, and a review of the genus: new *Goniopholis* from England. Zoological Journal of the Linnean Society 163:S66–S108.

Andrews, C. W. 1913a. A descriptive catalogue of the marine reptiles of the Oxford Clay. Part II. Bristish Museum, London.

Andrews, C. W. 1913b. On the skull and part of the skeleton of a crocodile from the middle Purbeck of Swanage, with a description of a new species (*Pholidosaurus laevis*, and a note on the skull of *Hylaeochampsa*. The Annals and Magazine of Natural History 11:485–494.

Brochu, C. A. 1999. Phylogenetics, taxonomy, and historical biogeography of Alligatoroidea. Journal of Vertebrate Paleontology 19:9–100.

Buckley, G. A., and C. A. Brochu. 1999. An enigmatic new crocodile from the Upper Cretaceous of Madagascar. Special Papers in Palaeontology 60:149–175.

Buffetaut, E. 1975. Sur l'anatomie et la position systématique de *Bernissartia fagesii* Dollo, L., 1883, crocodilien du Wealdien de Bernissart, Belgique. Bulletin de l'Institut Royal Des Sciences Naturelles de Belgique, Sciences de La Terre 51:1–20.

Buffetaut, E. 1982. Radiation évolutive, paléoécologie et biogéographie des crocodiliens mésosuchiens. Mémoires de La Société Géologique de France 142:1–88.

Buffetaut, E., and S. Hutt. 1980. *Vectisuchus leptognathus*, n.g., n.sp., a slender-snouted goniopholid crocodilian from the Wealden of the Isle of Wight. Neues Jahrbuch für Geologie und Paläeontologie, Monatshefte 7:385–390.

Buscalioni, A. D., P. Piras, R. Vullo, M. Signore, and C. Barbera. 2011. Early eusuchia crocodylomorpha from the vertebrate-rich Plattenkalk of Pietraroia (Lower Albian, southern Apennines, Italy). Zoological Journal of the Linnean Society 163:S199–S227.

Buscalioni, A. D., L. Alcalá, E. Espílez, and L. Mampel. 2013. European Goniopholididae from the Early Albian Escucha Formation in Ariño (Teruel, Aragón, Spain). Spanish Journal of Palaeontology 28:103–122.

Cope, E. D. 1875. Check-list of North American Batrachia and Reptilia with a systematic list of the higher groups and an essay on geographical distribution based on the specimens in the U.S. National Museum. Bulletin of the United States National Museum 1:1–104.

Dollo, L. 1883. Première note sur les crocodiliens de Bernissart. Bulletin de l'Institut Royal des Sciences Naturelles de Belgique 2:309–338.

Godefroit, P., J. Yans, and P. Bultynck. 2012. Bernissart and the Iguanodons: Historical perspective and new investigations; pp. 3–20 in Bernissart Dinosaurs and Early Cretaceous Terrestrial Ecosystems, Godefroit, P. (ed.). Indiana University Press.

Hooley, R. W. 1907. On the skull and greater portion of the skeleton of *Goniopholis crassidens* from the Wealden Shales of Atherfield (Isle of Wight). Quarterly Journal of the Geological Society of London 63:50–63.

Hua, S., E. Buffetaut, C. Legall, and P. Rogron. 2007. *Oceanosuchus boecensis* n. gen, n. sp., a marine pholidosaurid (Crocodylia, Mesosuchia) from the Lower Cenomanian of Normandy (western France). Bulletin de la Société Géologique de France 178:503–513.

Iordansky, N. N. 1973. The skull of the Crocodilia; pp. 201-262 in C. Gans and T.S. Parson (eds.), Biology of the Reptilia, vol. 1, morphology A. London and New New York.

Jouve, S., and D. Schwarz. 2004. *Congosaurus bequaerti*, a Paleocene dyrosaurid (Crocodyliformes; Mesoeucrocodylia) from Landana (Angola). Bulletin de

l'Institut Royal des Sciences Naturelles de Belgique, Sciences de la Terre 74:129–146.

Jouve, S., M. Iarochene, B. Bouya, and M. Amaghzaz. 2006. A new species of *Dyrosaurus* (Crocodylomorpha, Dyrosauridae) from the early Eocene of Morocco: phylogenetic implications. Zoological Journal of the Linnean Society 148:603–656.

Krebs, B. 1962. Ein *Steneosaurus*-Rest aus dem Oberen Jura von Dielsdorf, Kt. Zürich, Schweiz. Schweizerische Paläontologische Abhandlungen 79:1–28.

Lauprasert, K., G. Cuny, E. Buffetaut, V. Suteethorn, and K. Thirakhupt. 2007. *Siamosuchus phuphokensis*, a new goniopholidid from the Early Cretaceous (ante-Aptian) of northeastern Thailand. Bulletin de la Société Géologique de France 178:201–216.

Lortet, L. 1892. Les reptiles du bassin du Rhône. Archives du Muséum d'Histoire Naturelle de Lyon 5:3–133.

Martin, J. E. 2015. A sebecosuchian in a middle Eocene karst with comments on the dorsal shield in Crocodylomorpha. Acta Palaeontologica Polonica in press.

Martin, J. E., and M. Delfino. 2010. Recent advances in the comprehension of the biogeography of Cretaceous European eusuchians. Palaeogeography, Palaeoclimatology, Palaeoecology 293:406–418.

Martin, J. E., and E. Buffetaut. 2012. The maxillary depression of Pholidosauridae: an anatomical study. Journal of Vertebrate Paleontology 32:1442–1446.

Martin, J. E., K. Lauprasert, E. Buffetaut, R. Liard, and V. Suteethorn. 2014. A large pholidosaurid in the Phu Kradung Formation of north-eastern Thailand. Palaeontology 57:757–769.

Martin, J. E., T. Smith, F. de Lapparent de Broin, F. Escuillié, and M. Delfino. 2014. Late Palaeocene eusuchian remains from Mont de Berru, France, and the origin of the alligatoroid *Diplocynodon*. Zoological Journal of the Linnean Society 172:867–891.

Meers, M. B. 2003. Crocodylian forelimb musculature and its relevance to Archosauria. The Anatomical Record Part A 274A: 891–916.

Mook, C.C. 1921. Notes on the postcranial skeleton in the Crocodilia. Bulletin of the Aerican Museum of Natural History 44:67-100.

Owen, R. 1841. On British fossil reptiles. Report of the British Association for the Advancement of Science 11:60–204.

Owen, R. 1878. Monograph on the fossil Reptilia of the Wealden and Purbeck formations. Monograph of the Palaeontological Society 32:1–15.

Pol, D. 2005. Postcranial remains of *Notosuchus terrestris* (Archosauria: Crocodyliformes) from the upper Cretaceous of Patagonia, Argentina. Ameghiniana 42:1–17.

Pol, D. and Z. Gasparini. 2009. Skull anatomy of *Dakosaurus andiniensis* (Thalattosuchia: Crocodylomorpha) and the phylogenetic position of Thalattosuchia. Journal of Systematic Palaeontology 7: 163–197.

Pol, D., A. H. Turner, and M. A. Norell. 2009. Morphology of the Late Cretaceous crocodylomorph *Shamosuchus djadochtaensis* and a discussion of neosuchian phylogeny as related to the origin of Eusuchia. Bulletin of the American Museum of Natural History 324:1–103.

Pritchard, A. C., A. H. Turner, E. R. Allen, and M. A. Norell. 2013. Osteology of a North American goniopholidid (*Eutretauranosuchus delfsi*) and palate evolution in Neosuchia. American Museum Novitates 3783:1–56.

Puértolas-Pascual, E., J. I. Canudo, and L. M. Sender. 2015. New material from a huge specimen of *Anteophthalmosuchus* cf. *escuchae* (Goniopholididae) from the Albian of Andorra (Teruel, Spain): Phylogenetic implications. Journal of Iberian Geology 41.

Rogers, J. V. 2003. *Pachycheilosuchus trinquei* , a new procoelous crocodyliform from the Lower Cretaceous (Albian) Glen Rose Formation of Texas. Journal of Vertebrate Paleontology 23:128–145.

Salisbury, S. W. 2002. Crocodilians from the lower Cretaceous (Berriasian) Purbeck Limestone Group of Dorset, Southern England. Special Papers in Palaeontology 68:121–144.

Salisbury, S. W., and D. Naish. 2011. Crocodilians; pp. 305–369 in English Wealden Fossils, The Palaeontological Association. London.

Salisbury, S. W., and E. Frey. 2000. A biomechanical transformation model for the evolution of semi-spheroidal articulations between adjoining vertebral bodies in crocodilians; pp. 85–134 in C. C. Grigg, F. Seebacher and C. E. Franklin (eds.), Crocodilian biology and evolution. Surrey Beatty and Sons, Chipping Norton.

Salisbury, S. W., P. M. A. Willis, S. Peitz, and P. M. Sander. 1999. The crocodilian *Goniopholis simus* from the lower Cretaceous of north-western Germany. Special Papers in Palaeontology 60:121–148.

Salisbury, S. W., E. Frey, D. Martill, and M. C. Buchy. 2003. A new crocodilian from the Lower Cretaceous Crato Formation of north-eastern Brazil. Palaeontographica Abteilung A, Palaozoologie-Stratigraphie 270:3–47.

Salisbury, S. W., R. E. Molnar, E. Frey, and P. M. . Willis. 2006. The origin of modern crocodyliforms: new evidence from the Cretaceous of Australia. Proceedings of the Royal Society B: Biological Sciences 273:2439–2448.

Schwarz, D. 2002. A New Species of *Goniopholis* from the Upper Jurassic of Portugal. Palaeontology 45:185–208.

Schwarz, D., E. Frey, and T. Martin. 2006. The postcranial skeleton of the Hyposaurinae (Dyrosauridae; Crocodyliformes). Palaeontology 49:695–718.

Schwarz-Wings, D., E. Frey, and T. Martin. 2009. Reconstruction of the bracing system of the trunk and tail in hyposaurine dyrosaurids (Crocodylomorpha; Mesoeucrocodylia). Journal of Vertebrate Paleontology 29:453–472.

Sereno, P. C., H. C. Larsson, C. A. Sidor, and B. Gado. 2001. The giant crocodyliform *Sarcosuchus* from the Cretaceous of Africa. Science 294:1516–1519.

Sertich, J. J. W., and J. R. Groenke. 2010. Appendicular skeleton of *Simosuchus clarki* (Crocodyliformes: Notosuchia) from the Late Cretaceous of Madagascar. Journal of Vertebrate Paleontology 30:122–153.

Smith, D. K., E. R. Allen, R. K. Sanders, and K. L. Stadtman. 2010. A new specimen of *Eutretauranosuchus* (Crocodyliformes; Goniopholididae) from Dry Mesa, Colorado. Journal of Vertebrate Paleontology 30:1466–1477.

Turner, A. H. 2006. Osteology and phylogeny of a new species of *Araripesuchus* (Crocodyliformes: Mesoeucrocodylia) from the Late Cretaceous of Madagascar. Historical Biology 18:255–369.

Turner, A. H. 2015. A Review of *Shamosuchus* and *Paralligator* (Crocodyliformes, Neosuchia) from the Cretaceous of Asia. PLOS ONE 10:e0118116.

Turner, A. H., and A. C. Pritchard. 2015. The monophyly of Susisuchidae (Crocodyliformes) and its phylogenetic placement in Neosuchia. PeerJ 3:e759.

Westphal, F. 1962. Die Krokodilen des deutschen und englischen oberen Lias. Palaeontographica A 118:1–96.

Whetstone, K. N., and P. J. Whybrow. 1983. A “cursorial” crocodilian from the Triassic of Lesotho (Basutoland), southern Africa. Occasional Papers of the Museum of Natural History, University of Kansas 106:1–37.

Wilberg, E. W. 2015a. A new metriorhynchoid (Crocodylomorpha, Thalattosuchia) from the Middle Jurassic of Oregon and the evolutionary timing of marine adaptations in thalattosuchian crocodylomorphs. Journal of Vertebrate Paleontology 35:e902846.

Wilberg, E. W. 2015b. What’s in an outgroup? The impact of outgroup choice on the phylogenetic position of Thalattosuchia (Crocodylomorpha) and the origin of Crocodyliformes. Systematic Biology. In Press

Wu, X. C., D. B. Brinkman, and A. P. Russell. 1996a. A new alligator from the Upper Cretaceous of Canada and the relationship of early eusuchians. Palaeontology 39:351–376.

Wu, X.-C., D. B. Brinkman, and A. P. Russell. 1996b. *Sunosuchus junggarensis* sp.nov. (Archosauria: Crocodyliformes) from the Upper Jurassic of Xinjiang, People’s Republic of China. Canadian Journal of Earth Sciences 33:606–630.

Wu, X.-C., A. P. Russell, and S. L. Cumbaa. 2001. *Terminonaris* (Archosauria: Crocodyliformes): new material from Saskatchewan, Canada, and comments on its phylogenetic relationships. Journal of Vertebrate Paleontology 21:492–514.

Yans, J., J. Dejax, and J. Schnyder. 2012. On the age of the Bernissart iguanodons; pp. 79–86 in Bernissart Dinosaurs and Early Cretaceous Terrestrial Ecosystems, Godefroit, P. (Ed.). Indiana University Press.

Figures

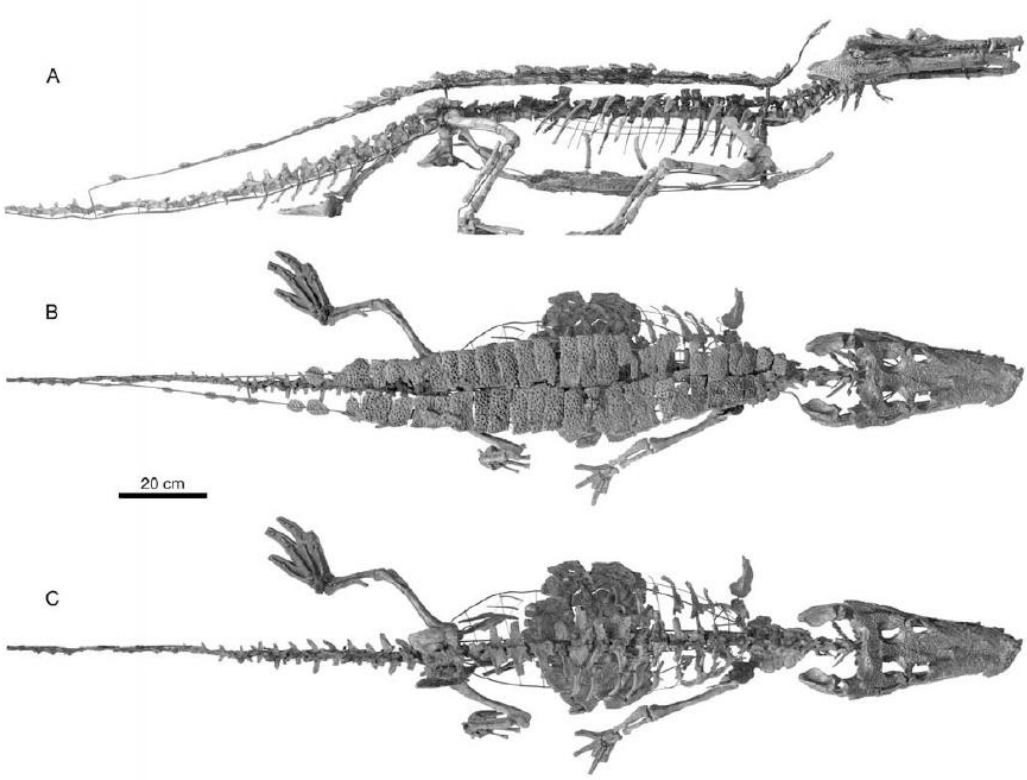

FIGURE 1. The mounted skeleton of *Anteophthalmosuchus hooleyi* (IRSNB R47) from the Barremian—Lower Aptian coal mine of Bernissart, Belgium in **A**, right lateral view; and dorsal view **B**, with and **C**, without shield of osteoderms.

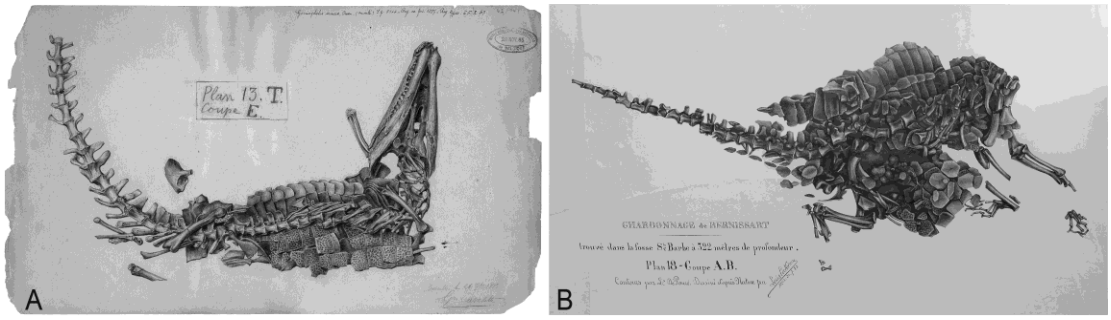

FIGURE 2. Historical drawings of the two specimens of *Anteophthalmosuchus hooleyi* from the Barremian—Lower Aptian coal mine of Bernissart. **A**, IRSNB R47 by Lavalette; **B**, IRSNB R290 by Cockelaere.

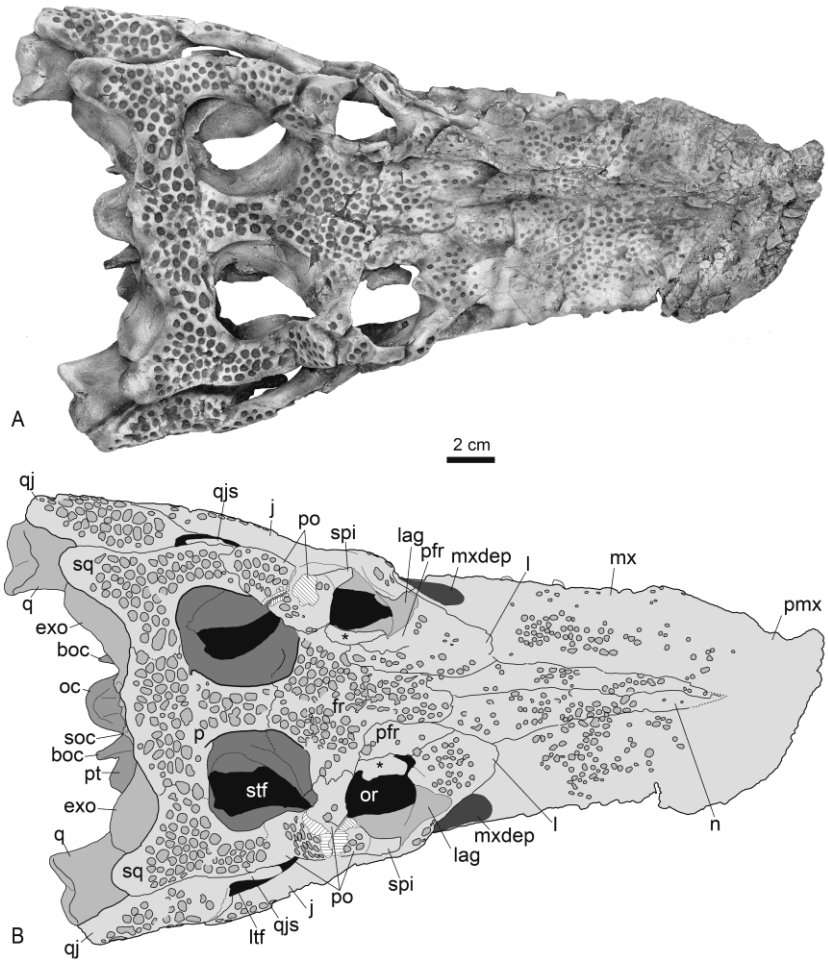

FIGURE 3. Photograph (**A**) and line drawing (**B**) of the dorsal view of the skull of *Anteophthalmosuchus hooleyi* (IRSNB R47). **Abbreviations: boc**, basioccipital; **exo**, exoccipital; **fr**, frontal; **j**, jugal; **l**, lacrimal; **lag**, lacrimal anterior groove; **ltf**, lower temporal fenestra; **mx**, maxilla; **mxdep**, maxillary depression; **n**, nasal; **oc**, occipital condyle; **or**, orbit; **p**, parietal; **pfr**, prefrontal; **pmx**, premaxilla; **po**, postorbital; **pt**, pterygoid; **q**, quadrate; **qj**, quadratojugal; **qjs**, quadratojugal spine; **soc**, supraoccipital; **spi**, postorbital spine; **stf**, supratemporal fenestra; *****, palpebral.

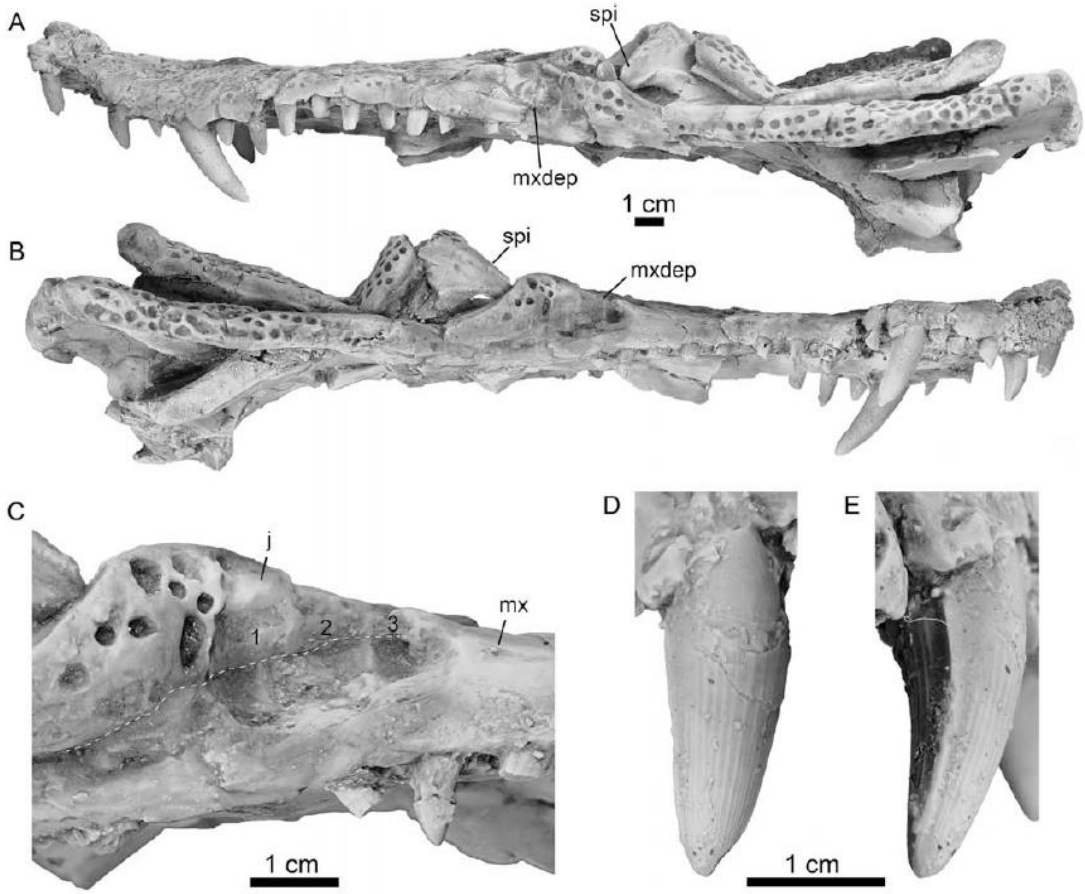

FIGURE 4. The skull of *Anteophthalmosuchus hooleyi* (IRSNB R47) from the Barremian—Lower Aptian coal mine of Bernissart, Belgium. **A**, left lateral view; **B**, right lateral view; **C**, right lateral view of the maxillary depression, the stipple line represents the maxillo-jugal suture; close-up of the fourth right maxillary tooth in **D**, labial and **E**, distal views. **Abbreviations: 1–3**, individual spaces in the maxillary depression; **j**, jugal; **mx**, maxilla; **mxdep**, maxillary depression; **spi**, postorbital spine.

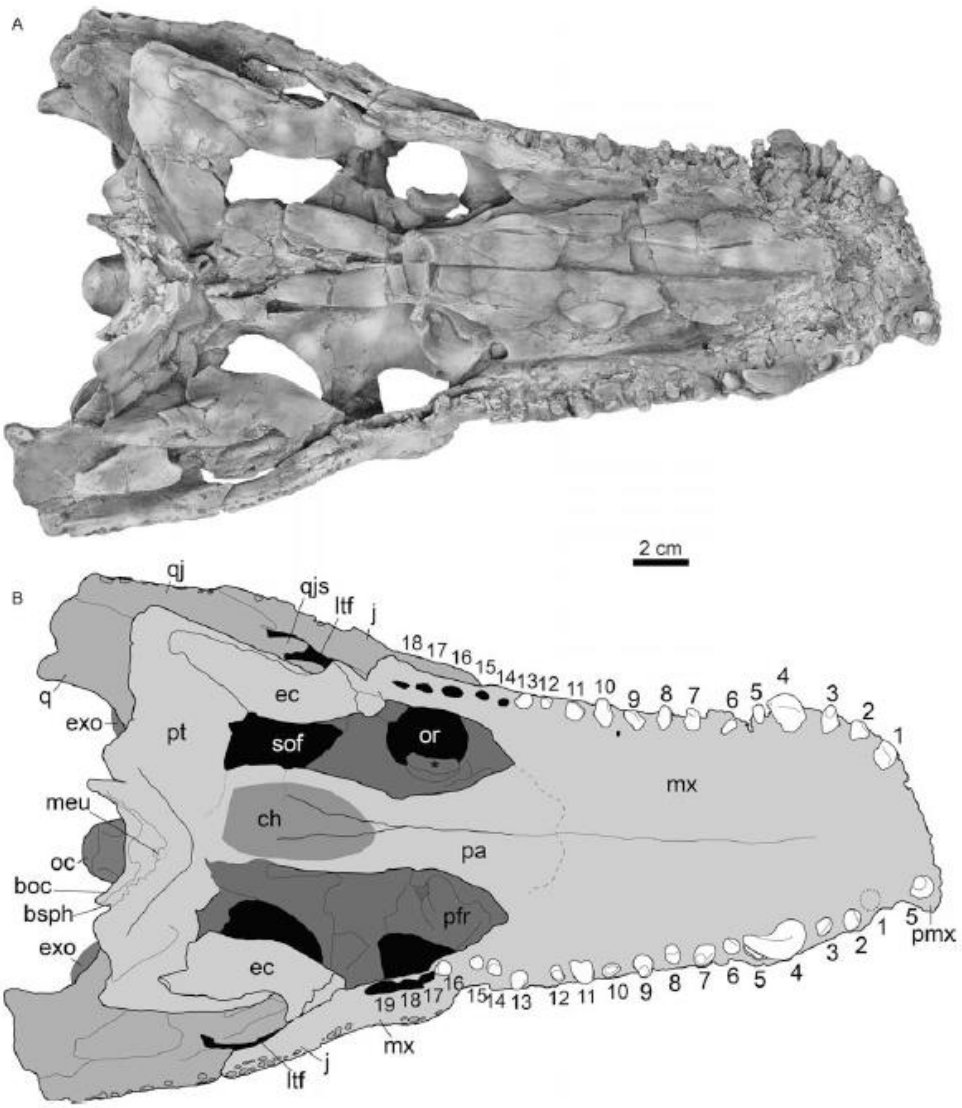

FIGURE 5. Photograph (**A**) and line drawing (**B**) of the ventral view of the skull of *Anteophthalmosuchus hooleyi* (IRSNB R47). **Abbreviations: boc**, basioccipital; **bsph**, basisphenoid; **ch**, choanae; **ec**, ectopterygoid; **exo**, exoccipital; **j**, jugal; **ltf**, lower temporal fenestra; **meu**, median Eustachian foramen; **mx**, maxilla; **oc**, occipital condyle; **or**, orbit; **pmx**, premaxilla; **pt**, pterygoid; **q**, quadrate; **qj**, quadratojugal; **qjs**, quadratojugal spine; **sof**, suborbital fenestra; *****, palpebral.

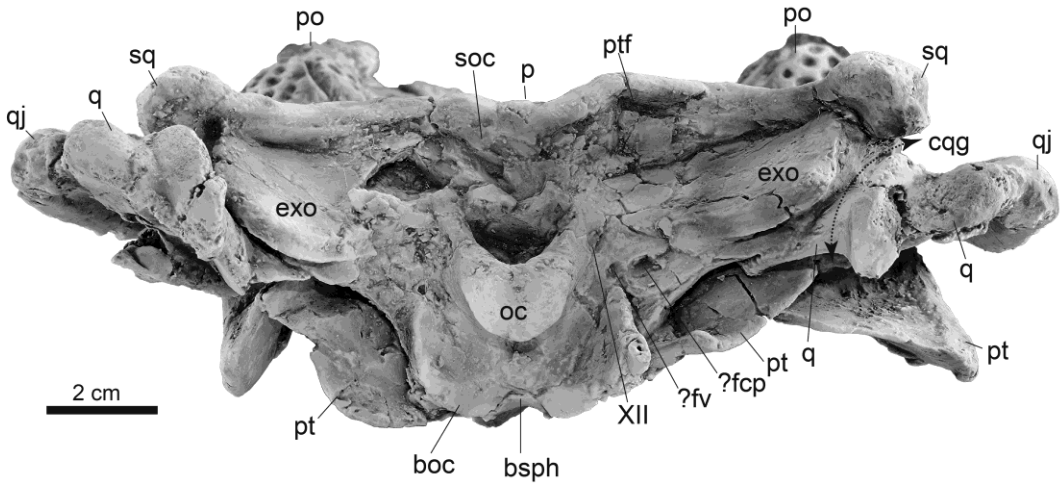

FIGURE 6. Occipital view of the skull of *Anteophthalmosuchus hooleyi* (IRSNB R47). **Abbreviations**: **boc**, basioccipital; **bsph**, basisphenoid; **cqg**, cranioquadrate groove; **exo**, exoccipital; **?fcp**, foramen caroticus posterius; **?fv**, foramen vagus; **oc**, occipital condyle; **p**, parietal; **po**, postorbital; **pt**, pterygoid; **ptf**, posttemporal fenestra; **q**, quadrate; **qj**, quadratojugal; **soc**, supraoccipital; **sq**, squamosal; **XII**, opening for hypoglossal foramen.

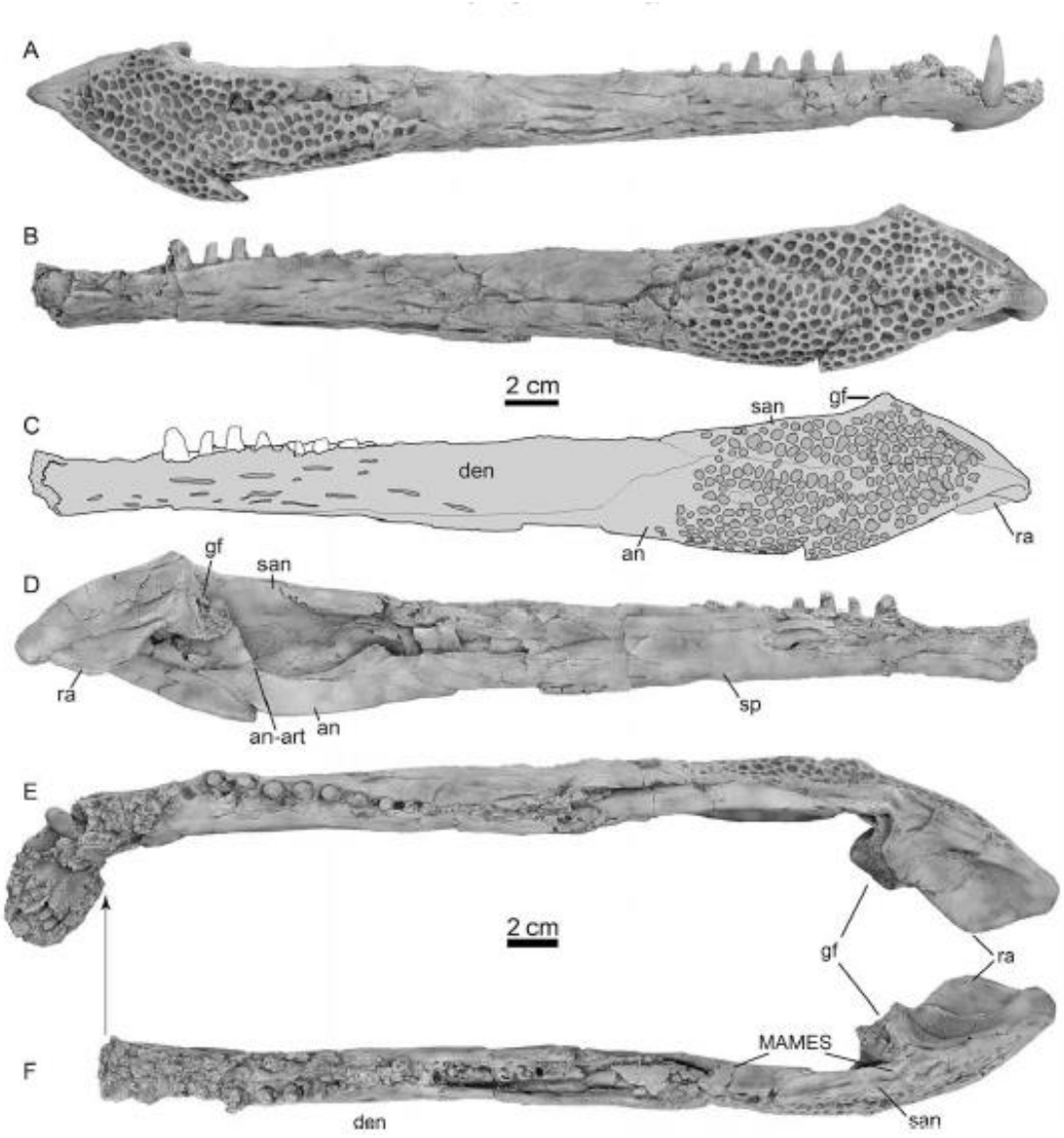

FIGURE 7. The mandible of *Anteophthalmosuchus hooleyi* (IRSNB R47). Right mandibular ramus in **A**, lateral view; left mandibular ramus in **B**, lateral view with **C**, corresponding line drawing; **D**, medial view of right ramus and **E** and **F**, occlusal views of right and left rami, respectively. The arrow indicates the match between both rami along their break. **Abbreviations: an**, angular; **den**, dentary; **gf**, glenoid fossa; **MAME**, insertion for M. adductor mandibulae externus; **san**, surangular; **ra**, retroarticular process.

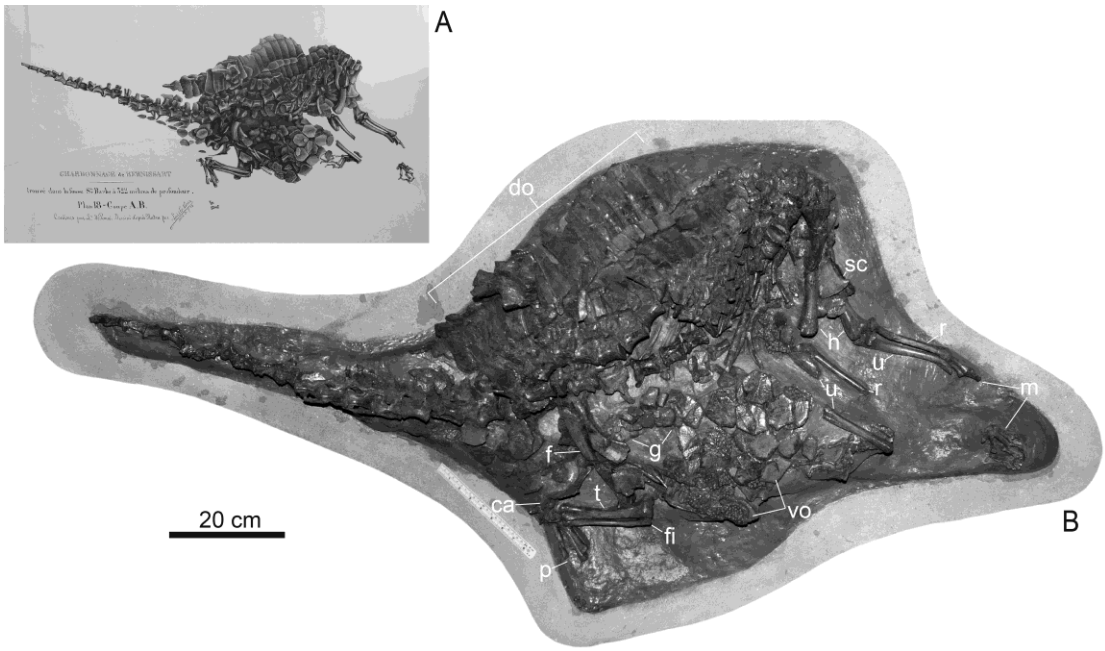

FIGURE 8. The articulated skeleton of *Anteophthalmosuchus hooleyi* (IRSNB R290) from the Barremian—Lower Aptian coal mine of Bernissart, Belgium still encased in sediment. Inset drawing by Cockelaere.

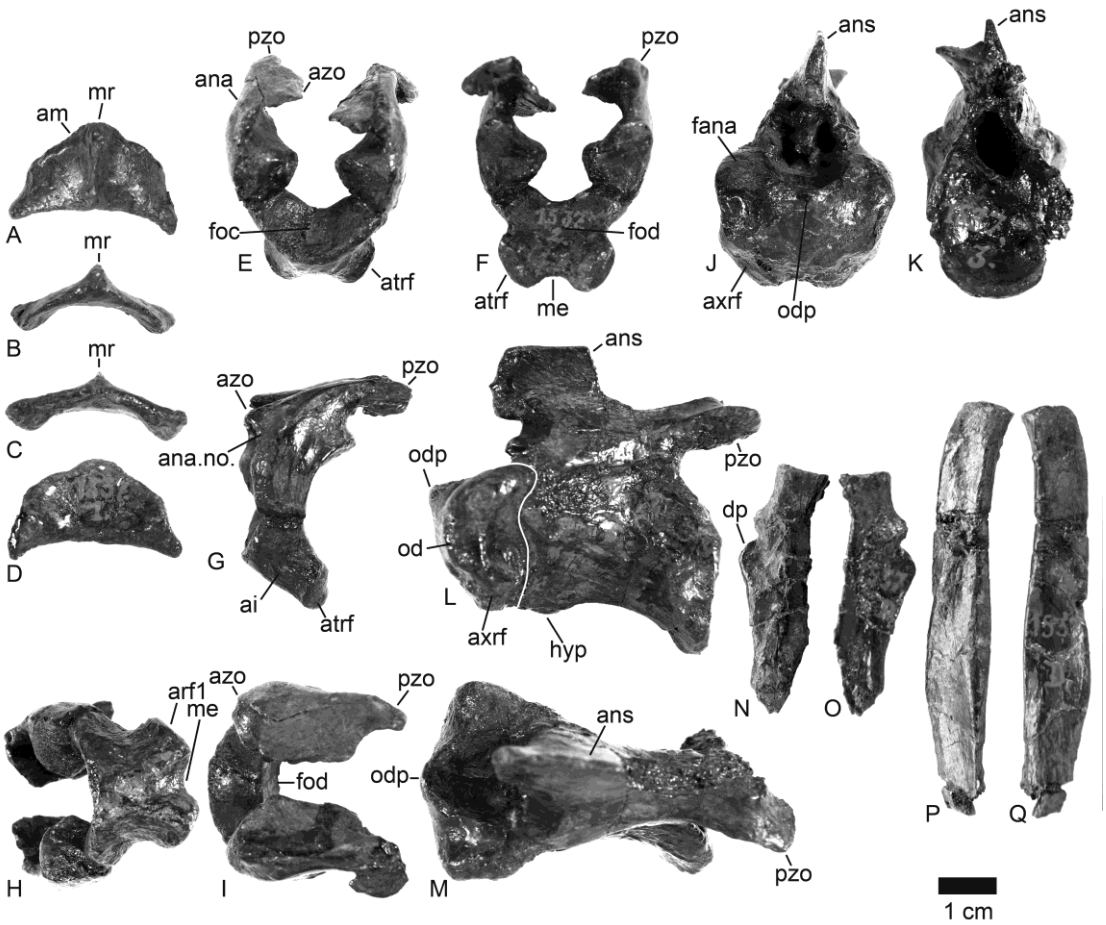

FIGURE 9. Disarticulated elements of the atlas-axis complex of *Anteophthalmosuchus hooleyi* (IRSNB R47) from the Barremian—Lower Aptian coal mine of Bernissart, Belgium. Proatlas in **A**, dorsal, **B**, anterior, **C**, posterior, **D**, ventral views. Atlas in **E**, anterior, **F**, posterior, **G**, left lateral, **H**, ventral, **I**, dorsal views. Axis in **J**, anterior, **K**, posterior, **L**, left lateral, **M**, dorsal views. In **L**, the white line delineates the odontoid from the axis centrum. Right axial rib in **N**, lateral, **O**, medial views; right atlantal rib in **P**, lateral, **Q**, medial views. **Abbreviations: am**, anterior margin of proatlas; **ana**, atlas neural arch; **ana.no.**, notch on atlas neural arch; **ans**, axis neural spine; **atrf**, atlantal rib facet; **axrf**, axial rib facet; **azo**, pre-zygapophysis; **dp**, dorsal process; **foc**, facet for occipital condyle; **fod**, facet for odontoid process; **hyp**, hypapophysis; **me**, median excavation of atlas; **mr**, median ridge of proatlas; **od**, odontoid; **odp**, odontoid process; **pzo**, post-zygapophysis.

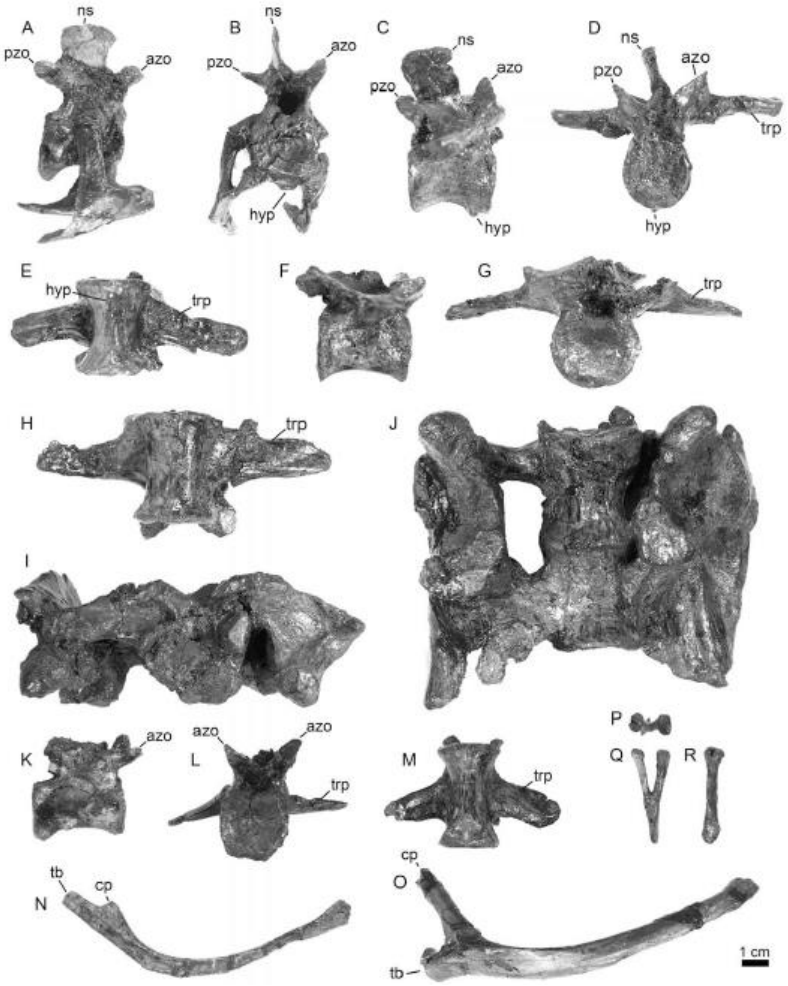

FIGURE 10. Selected elements of the axial skeleton of *Anteophthalmosuchus hooleyi* (IRSNB R47) from the Barremian—Lower Aptian coal mine of Bernissart, Belgium. Third cervical vertebra in **A**, right lateral; **B**, anterior views; third thoracic vertebra in **C**, right lateral; **D**, anterior; **E**, ventral views; fourteenth thoracic vertebra in **F**, right lateral; **G**, anterior; **H**, ventral views; sacrum in **I**, anterior; **J**, ventral views; third caudal vertebra in **K**, right lateral; **L**, anterior; **M**, ventral views; **N**, tenth thoracic rib in anterior view; **O**, second thoracic rib in anterior view; chevron in **P**, proximal; **Q**, anterior; **R**, lateral views. **Abbreviations: azo**, pre-zygapophysis; **cp**, capitulum; **dp**, dorsal process; **hyp**, hypapophysis; **ns**, neural spine; **pzo**, post-zygapophysis; **tb**, tuberculum; **trp**, transverse process.

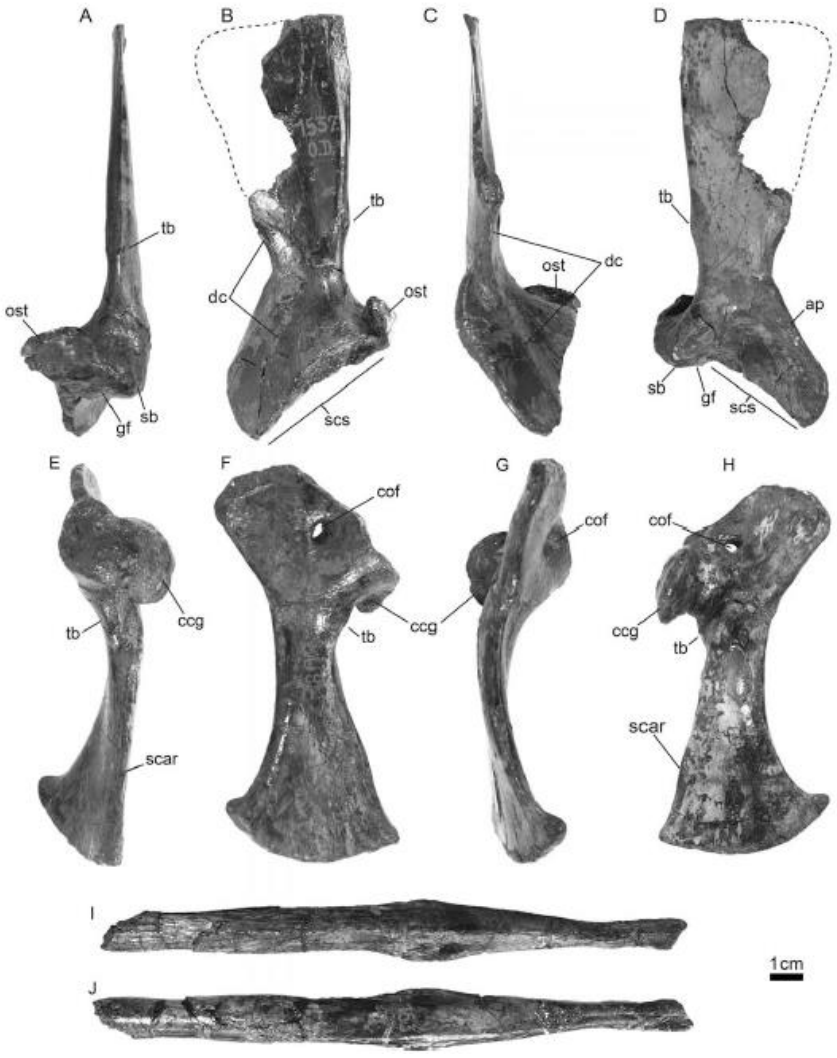

FIGURE 11. The right shoulder girdle of *Anteophthalmosuchus hooleyi* (IRSNB R47) from the Barremian—Lower Aptian coal mine of Bernissart, Belgium. Scapula in **A**, posterior; **B**, medial; **C**, anterior; **D**, lateral views. Coracoid in **E**, posterior; **F**, medial; **G**, anterior; **H**, lateral views; Interclavicle in **I**, dorsal and **J**, ventral views. **Abbreviations: ap**, acromion process; **ccg**, coracoid contribution to glenoid; **cof**, coracoid foramen; **dc**, deltoid crest; **gf**, glenoid fossa; **ost**, osteoderm; **sb**, supraglenoid buttress; **scs**, scapular synchondrosis; **tb** tubercle for M. triceps brachii.

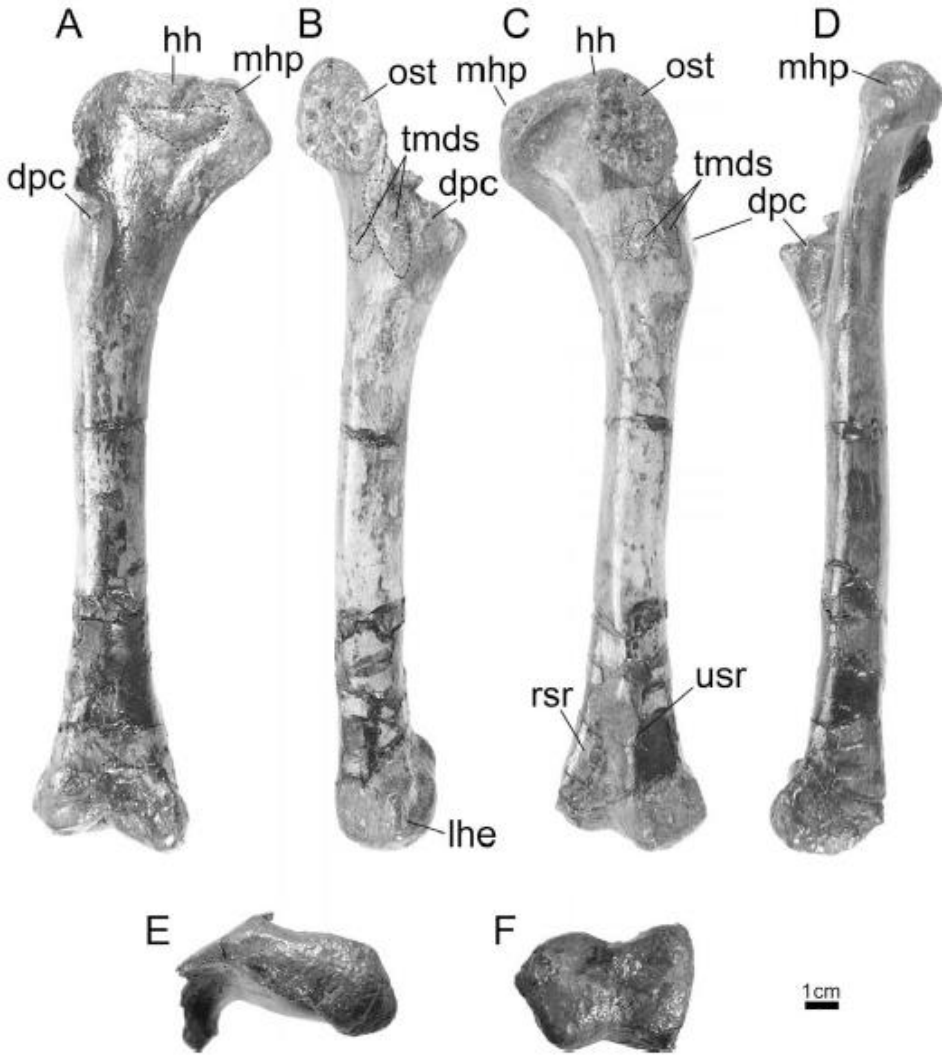

FIGURE 12. The right humerus of *Anteophthalmosuchus hooleyi* (IRSNB R47) from the Barremian—Lower Aptian coal mine of Bernissart, Belgium. Humerus in **A**, anterior; **B**, lateral; **C**, posterior; **D**, medial views. Ulna (**E**, **F**, **G**) and radius (**I**, **J**, **K**) in **E**, posterior; **F**, medial; **G**, anterior; **H**, lateral; **I**, posterior, **J**, medial; **K**, anterior. **Abbreviations: dpc**, deltopectoral crest; **hh**, humeral head; **lhe**, lateral humeral epicondyle; **mhp**, medial humeral process; **ost**, osteoderm; **rsr**, radial supracondylar ridge; **tmds**, insertion point for M. teres major and M. dorsalis scapulae; **usr**, ulnar supracondylar ridge.

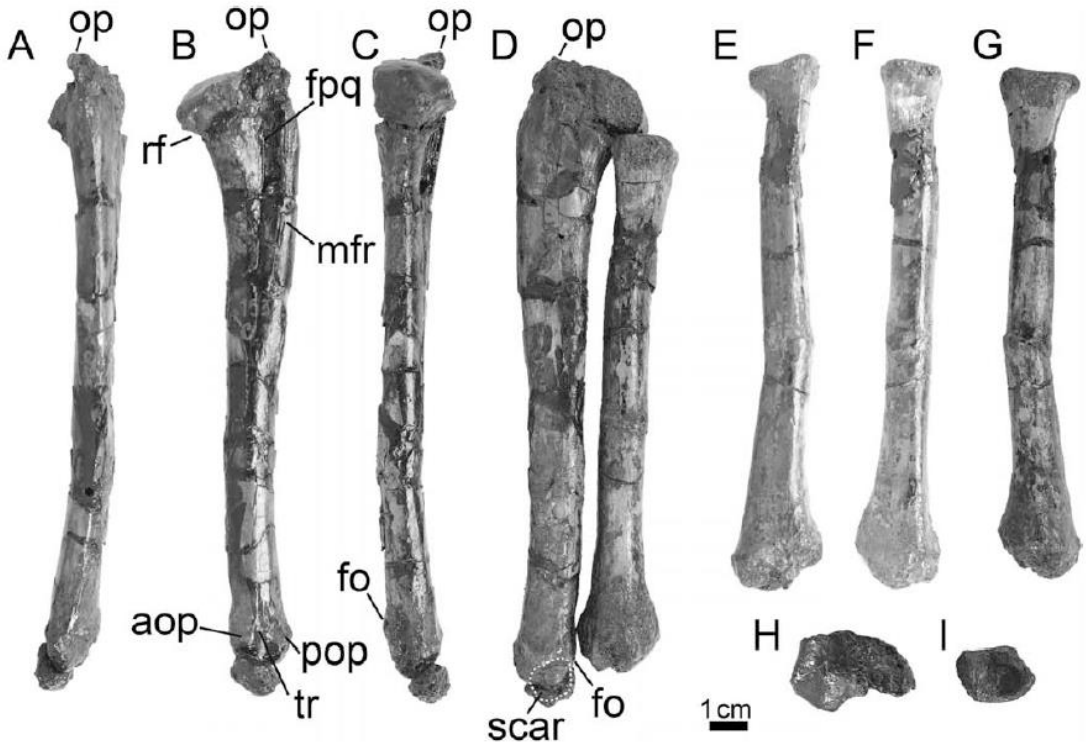

FIGURE 13. Elements of the right forelimb of *Anteophthalmosuchus hooleyi* (IRSNB R47) from the Barremian—Lower Aptian coal mine of Bernissart, Belgium. Ulna (**A**, **B**, **C, H**) and radius (**E**, **F**, **G, I**) in **A**, posterior; **B**, medial; **C**, anterior; **D**, lateral; **E**, posterior, **F**, medial; **G**, anterior; **H**, **I**, proximal views. **Abbreviations: aop**, anterior oblique process; **fpq**: fossa for pronator quadratus; **fo**, foramen; **mfr**, medial flexor ridge; **op**, olecranon process; **pop**, posterior oblique process; **rf**, radial facet; **tr**, trochlea.

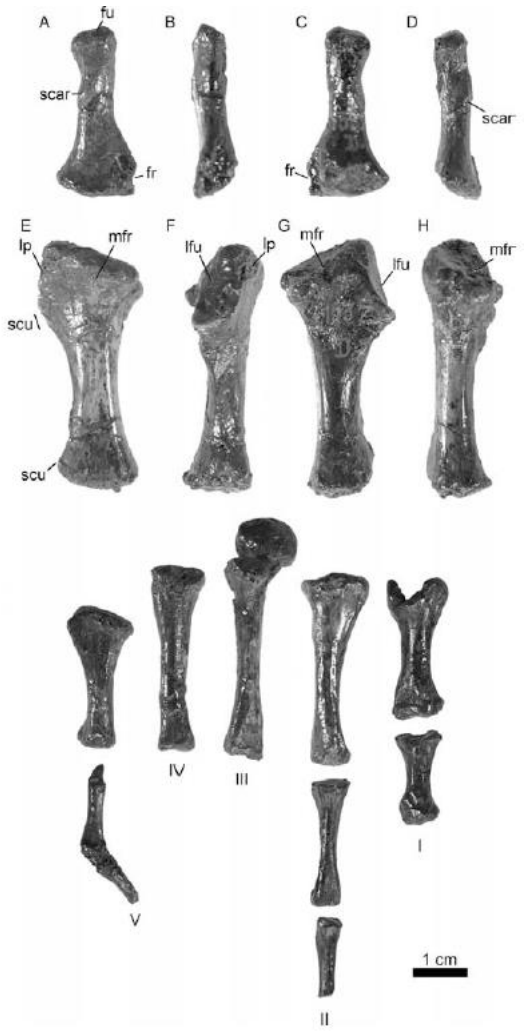

FIGURE 14. The right ulnare and radiale of *Anteophthalmosuchus hooleyi* (IRSNB R47) from the Barremian—Lower Aptian coal mine of Bernissart, Belgium. Ulnare in **A**, anterior; **B**, lateral; **C**, posterior; **D**, medial views. Radiale in **E**, anterior; **F**, lateral; **G**, posterior; **H**, medial views. **I to V**, ordered digits of the right manus as preserved. **Abbreviations: fr**, facet for radiale; **fu**, facet for ulna; **lfu**, lateral facet for ulna; **lp**, lateral process; **mfr**, medial facet for radius; **scu**, small contact for ulnare.

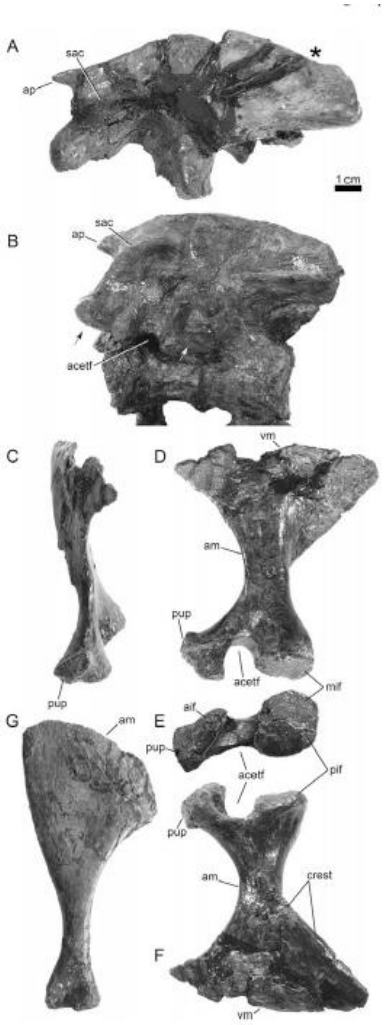

FIGURE 15. The pelvic girdle of *Anteophthalmosuchus hooleyi* (IRSNB R47) from the Barremian—Lower Aptian coal mine of Bernissart, Belgium. Right Ilium in **A**, lateral view (flipped to ease comparison); left ilium in **B**, lateral view; ischium in **C**, posterior; **D**, medial; **E**, proximal; **F**, lateral views. Pubis in **G**, dorsal view. The star symbol indicates the wasp-waisted margin on the distal blade of the right ilium. Arrows point to the peduncles on the ilium, which articulate with the ischium. **Abbreviations: acetf**, acetabulum foramen; **aif**, anterior iliac facet; **am**, anterior margin; **ap**, anterior process; **mif**, medial iliac facet; **pif**, posterior iliac facet; **pup**, pubic process; **sac**, supraacetabular crest; **vm**, ventral margin.

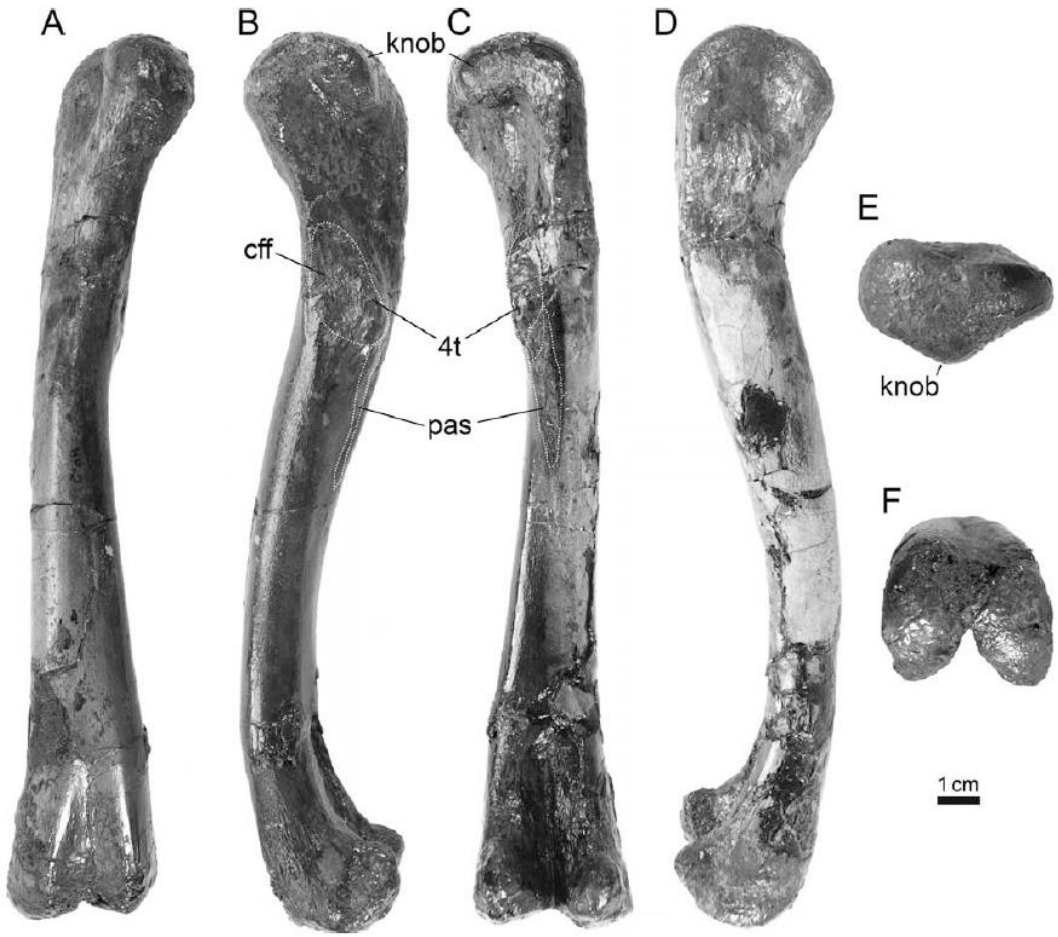

FIGURE 16. The right femur of *Anteophthalmosuchus hooleyi* (IRSNB R47) from the Barremian—Lower Aptian coal mine of Bernissart, Belgium in **A**, anterior; **B**, medial; **C**, posterior; **D**, lateral views. **Abbreviations: cff**, caudofemoralis flange; **pas**, primary adductor scar; **4t**, fourth trochanter.

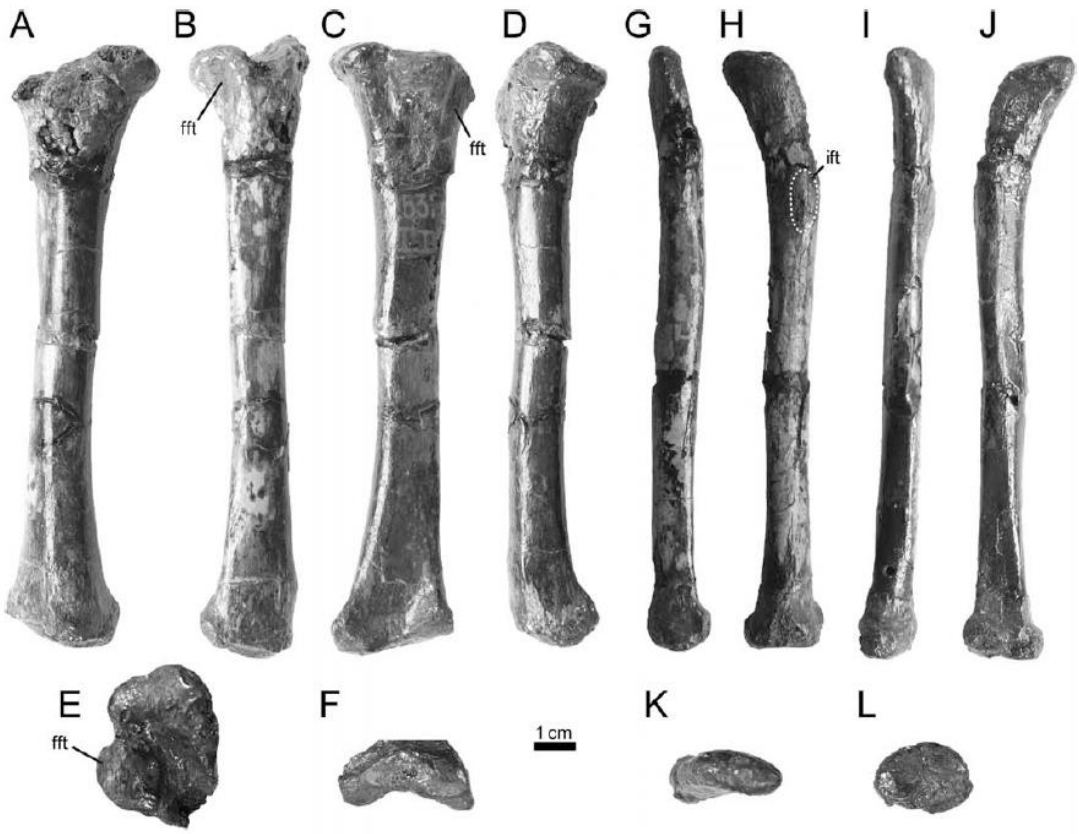

FIGURE 17. Elements of the right hind limb of *Anteophthalmosuchus hooleyi* (IRSNB R47) from the Barremian—Lower Aptian coal mine of Bernissart, Belgium. Tibia in **A**, anterior; **B**, lateral; **C**, posterior; **D**, medial; **E**, proximal and **F**, distal views. Fibula in **G**, anterior; **H**, lateral; **I**, posterior; **J**, medial; **K**, proximal and **L**, distal views. **Abbreviations: fft**, proximal fibular facet of tibia; **ift**, iliofibularis trochanter.

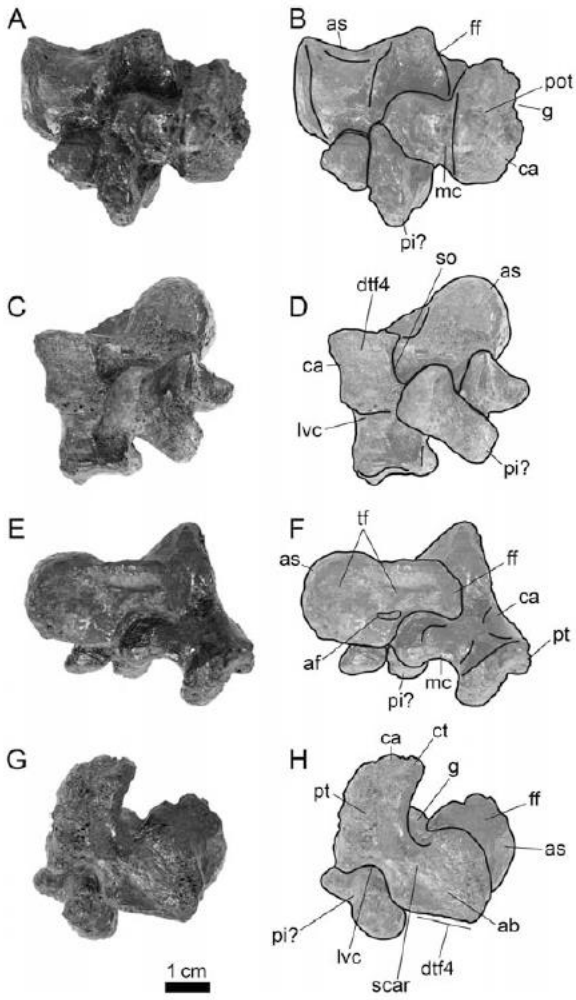

FIGURE 18. Astragalus and calcaneum of *Anteophthalmosuchus hooleyi* (IRSNB R47) from the Barremian—Lower Aptian coal mine of Bernissart, Belgium in **A, B**, posterior; **C, D**, ventral; **E, F**, dorsal; **G, H**, lateral views. **Abbreviations: ab**, anterior ball; **af**, astragalar fossa; **as**, astragalus; **ca,** calcaneum; **ct**, calcaneal tuber; **dtf4**, distal tarsal facet 4; **ff**, fibular facet; **g**, groove 1; **lvc**, lateroventral channel; **mc**, medial chanel; **pt**, posterior tuber; **so,** socket; **tf**, tibial facet.

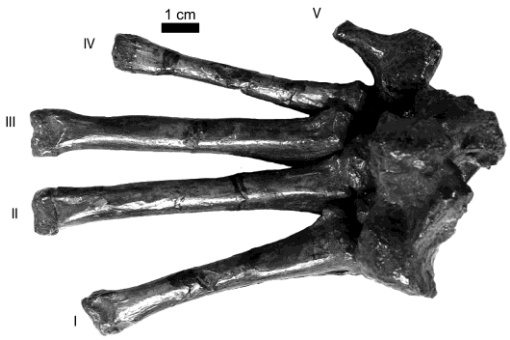

FIGURE 19. The right pes of *Anteophthalmosuchus hooleyi* (IRSNB R47) from the Barremian—Lower Aptian coal mine of Bernissart, Belgium in dorsal view with ordered digit positions **I** to **V** as preserved.

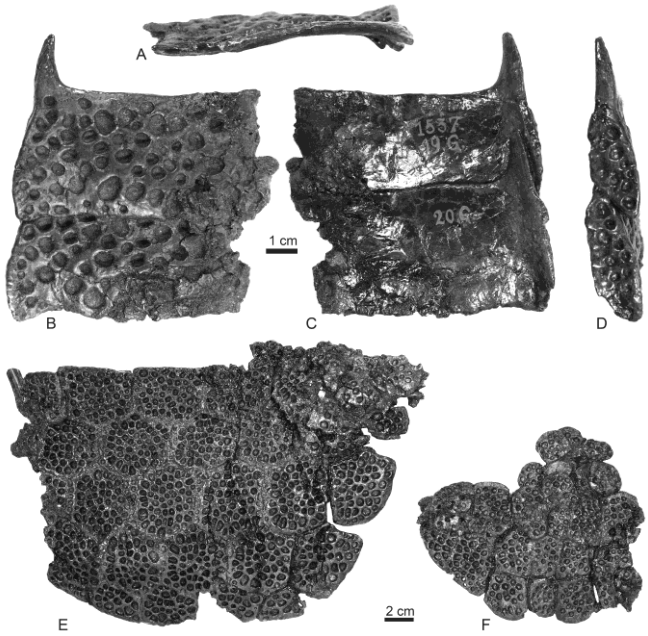

FIGURE 20. Selected elements of the shield of *Anteophthalmosuchus hooleyi* (IRSNB R47) from the Barremian—Lower Aptian coal mine of Bernissart, Belgium. Articulated left dorsal osteoderms of the mid-trunk region in **A**, anterior; **B**, dorsal; **C**, ventral and **D**, lateral views. Slabs of articulated ventral osteoderms showing **E**, the polygonal morphology of central elements and **F**, and the trapezoideal outline of peripheral elements.

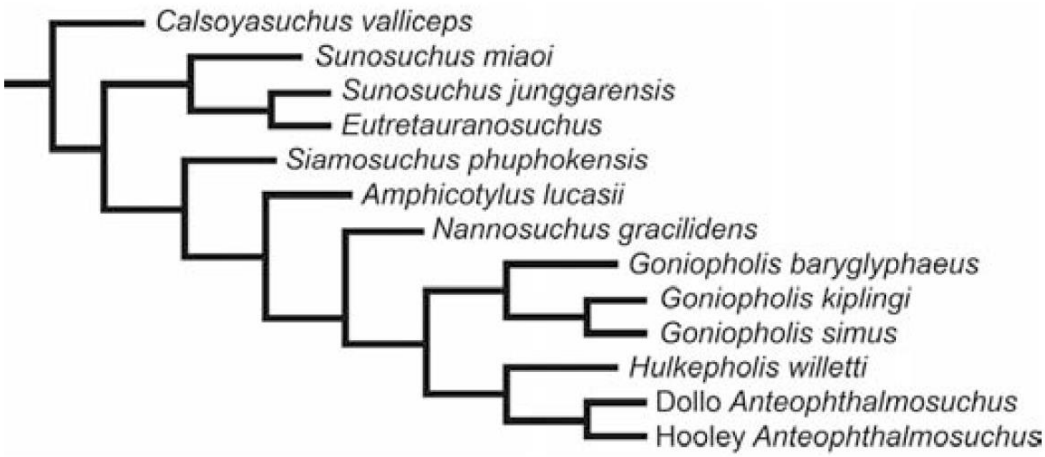

FIGURE 21. Strict consensus tree of the phylogenetic analysis conducted on the datamatrix of Andrade et al. (2011), confirming the phylogenetic position of *Anteophthalmosuchus hooleyi* within Goniopholididae as well as supporting the affiliation of the Dollo specimen to that species. Note that only the intrarelationships of Goniopholididae are presented.

TAB 1. Checklist of European goniopholidids recognized in this paper.

Taxon	Holotype	Provenance(s)	Age	References
Goniopholis crassidens	NHMUK 3798 (lectotype)	Purbeck Limestone Group of Swanage, England	Berriasian	Owen (1841); Salisbury (2002); Salisbury and Naish (2011)
Goniopholis simus	NHMUK 41098	Purbeck Limestone Group of Swanage, England and Niedersachsen Basin, northwestern Germany	Berriasian	Owen (1878); Salisbury et al. (1999); Salisbury (2002)
Goniopholis baryglyphaeus	IPFUB Gui Croc 1	Alcobaça Formation of Guimarota coal mine, Leiria, Portugal	Kimmeridgian	Schwarz (2002)
Goniopholis kiplingi	DORCM 12154	Intermarine beds (bed 129b), Purbeck Limestone Group of Durlstone Bay, Swanage, England	Berriasian	Andrade et al. (2011)
Nannosuchus gracilidens	NHMUK 48217	Beccles residuary marls, Durlston Bay, England	Berriasian	Owen (1879); Salisbury (2002)
Vectisuchus leptognathus	SMNS 50984	Upper Wessex Formation of Barnes High, Isle of Wight, England	Barremian	Buffetaut and Hutt (1980); Salisbury and Naish (2011)
Hulkepholis willetti	BMNHB 001876	Grinstead Formation of Cuckfield, West Sussex, England	Berriasian	Hulke (1878); Salisbury and Naish (2011); Buscalioni et al. (2013)
Hulkepholis plotos	AR-1/56	Escucha Formation of site AR-1, Mina Santa María, Ariño, Teruel Province, Spain	Albian	Buscalioni et al. (2013)
Anteophthalmosuchus hooleyi	NHMUK R3876	Vectis Formation of Atherfield Point and Wessex Formation, Isle of Wight, England; coal mine at Bernissart, Belgium	Barremian/Aptian	Salisbury and Naish (2011); this study
Anteophthalmosuchus escuchae	AR-1/37	Escucha Formation of site AR-1, Mina Santa María, Ariño, Teruel Province, Spain	Albian	Buscalioni et al. (2013); Puértolas-Pascual et al. (2015)

TAB 2. Dimensions (in cm) of *Anteophthalmosuchus hooleyi*,

IRSNB R47.

Length of skull from premaxillary-maxillary notch to posterior edge of cranial table	27.2
Maximal width of skull, across quadratojugals	18.9
Length of snout (to premaxillary-maxillary notch)	16
Length of post-snout region, from anterior border of orbit to posterior edge of cranial table	11.2
Maximal width of snout (at largest mx tooth)	8.8
Maximal length of orbit (right)	3
Maximal width of orbit (right)	3
Interorbital width	5.2
Length of cranial table, through center of supratemporal fenestrae (right)	8
Width of cranial table, across centers of supratemporal fenestrae	13.5
Maximal length of supratemporal fenestra (left / right)	4.7 / 4.4
Maximal width of supratemporal fenestra	4
Spine anterior tip–postorbital bar distance	?
Anteroposterior thickness of postorbital bar	1.5
Interfenestral (supratemporal fenestra) width	1.7
Length of ventral border of infratemporal fenestra (left)	4.2
Length of long axis of suborbital fenestra (left / right)	11 / 10.1
Length of short axis of suborbital fenestra (left / right)	4 / 3.2
Interfenestral width of palatines at mid-length	2.8
Width of choanae	<3
Width across pterygoid flanges	>14